ChemPubSoc Europe

DOI: 10.1002/chem.201405599

CHEMISTRY A European Journal Full Paper

Conformation Analysis | *Hot Paper*

Conformational Dependence of Through-Space Tellurium–Tellurium Spin–Spin Coupling in *Peri*-Substituted Bis(Tellurides)

Fergus R. Knight, Louise M. Diamond, Kasun S. Athukorala Arachchige, Paula Sanz Camacho, Rebecca A. M. Randall, Sharon E. Ashbrook, Michael Bühl, Alexandra M. Z. Slawin, and J. Derek Woollins*[a]

Abstract: Three related series of *peri*-substituted bis(tellurides) bearing naphthalene, acenaphthene and acenaphthylene backbones (Nap/Acenap/Aceyl$(TeY)_2$ (Nap = naphthalene-1,8-diyl **N**; Acenap = acenaphthene-5,6-diyl **A**; Aceyl = acenaphthylene-5,6-diyl **Ay**; Y = Ph **1**; Fp **2**; Tol **3**; An-*p* **4**; An-*o* **5**; Tp **6**; Mes **7**; Tip **8**) have been synthesised and their solid-state structures determined by X-ray crystallography. Molecular conformations were classified as a function of the two C9-C-Te-C(Y) dihedral angles (θ); in the solid all members adopt AB or CC*t* configurations, with larger Te(aryl) moieties exclusively imposing the CC*t* variant. Exceptionally large $J(^{125}Te,^{125}Te)$ spin–spin coupling constants between 3289–3848 Hz were obtained for compounds substituted by bulky Te(aryl) groups, implying these species are locked in a CC*t*-type conformation. In contrast, compounds incorporating smaller Te(aryl) moieties are predicted to be rather dynamic in solution and afford much smaller *J* values (2050–2676 Hz), characteristic of greater populations of AB conformers with lower couplings. This conformational dependence of through-space coupling is supported by DFT calculations.

Introduction

Spin–spin coupling constants (SSCCs) provide valuable information about the environment surrounding coupled atomic nuclei within a molecule and are becoming an increasingly important tool for analysing structures. The extent of spin–spin coupling is governed by the amount of contact between nuclear magnetic dipoles and gives an insight into the underlying connectivity and spacial arrangement of the coupled atoms.[1–4] Indirect (scalar) coupling is transmitted by the intervening network of bonds linking the coupled nuclei (through-bond coupling) and is thus dependent upon the degree of s-orbital participation in the bonding and the polarisability of the s-electrons. Through-bond coupling naturally recedes as additional bonds are added and the nuclei become more detached, with coupling through more than four bonds rarely observed.[1–4]

Nevertheless, when NMR active atomic nuclei are forced to lie within the sum of their van der Waals radii, but still remain many bonds apart (formally non-bonded), additional coupling can be transmitted through the interaction of overlapping lone-pair orbitals (through-space coupling), leading to uncharacteristically large *J* values for formally four-bond (^4J) and even longer coupling.[1,4–9] Naturally, the extent of through-space spin–spin coupling is determined by the strength of the lone-pair interaction, which relies on the efficient overlap of orbitals, and is thus strongly dependent on the internuclear distance.[1–4]

Several studies of $J(^{19}F,^{19}F)$ SSCCs have been undertaken to try and quantify the dependency of through-space J_{FF} coupling and the intramolecular non-bonding distance d_{FF}.[5–7] For example, Mallory and co-workers derived an exponential correlation of d_{FF} and J_{FF} for a series of 1,8-difluoronaphthalenes (**A**&**B**; Figure 1) which exhibit exceptionally large $J(^{19}F,^{19}F)$ SSCCs in the range 65–85 Hz.[6] In these compounds, the exocyclic C–F bonds are coplanar and align virtually parallel, resulting in F···F separations of around 2.58 Å (r_{vdW}(F) 1.35 Å).[10] Interestingly, the 1,8-difluoroacenaphthylenes investigated as part of the study, containing a semi-rigid unsaturated ethene bridge, did not conform to the correlation and were subsequently omitted. Acenaphthenes with significant double bond character associated with their saturated ethane linkers similarly afforded anomalous J_{FF} values and were also excluded. The deviation observed for these derivatives compared to the remaining members of the series was attributed to the difference in aromaticity of the acenaphthylene backbone and a greater interaction between the fluorine lone-pair orbitals and the π-system. Confirmed by a later DFT study, the elevated J_{FF} values resulted from a greater through-bond contribution to the overall coupling due to the increased π-interactions, subsequently causing the observed deviation from the d_{FF}/J_{FF} exponential curve.[6]

[a] *Dr. F. R. Knight, Dr. L. M. Diamond, Dr. K. S. A. Arachchige, P. Sanz Camacho, R. A. M. Randall, Prof. S. E. Ashbrook, Prof. M. Bühl, Prof. A. M. Z. Slawin, Prof. J. D. Woollins*
EaStCHEM School of Chemistry and Centre for Magnetic Resonance
University of St Andrews
St Andrews, KY16 9ST (UK)
E-mail: jdw3@st-andrews.ac.uk

Supporting information for this article is available on the WWW under http://dx.doi.org/10.1002/chem.201405599.

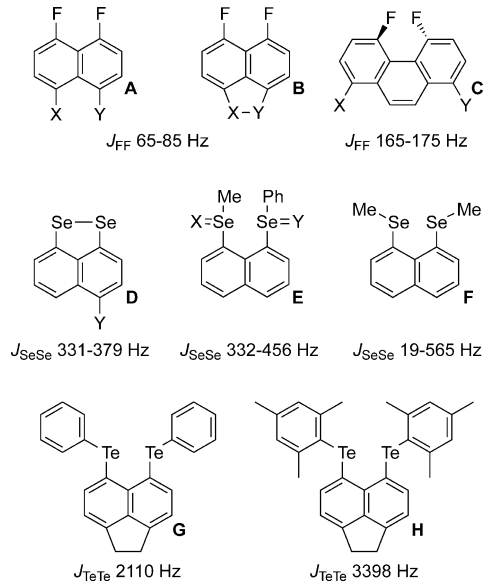

Figure 1. Systems exhibiting through-space spin–spin coupling between closely aligned, but formally non-bonded NMR active nuclei.

Whilst the efficiency of lone-pair orbital overlap, and the magnitude of through-space coupling, is greatly influenced by the non-bonded internuclear distance, it is also sensitive to the angular orientation of the overlapping lone-pairs. For instance, 4,5-difluorophenanthrene derivatives of type **C** (Figure 1), in which the exocyclic C—F bonds are no longer coplanar, nor parallel, produce much larger $J(^{19}F,^{19}F)$ SSCCs than their naphthalene equivalents, with J values of 165–175 Hz truly massive for formally five-bond ($^5J_{FF}$) couplings.[6]

With the aid of quantum-chemical computations, torsional angular dependence of $^1J(^{77}Se,^{77}Se)$ spin–spin coupling has been predicted in a model diselenide, MeSeSeMe, justifying the substantial J values (331–379 Hz) observed experimentally for restricted naphtho[1,8-*c*,*d*]-1,2-diselenoles of type **D** (Figure 1).[9] In the same study, substantial $^4J(^{77}Se,^{77}Se)$ coupling constants of equivalent or even greater magnitude were reported for naphthalenes containing non-bonded Se···Se (332 Hz) and O=Se···Se=O (456 Hz) interactions (**E**, Figure 1), the latter the largest known ^4J-coupling between formally non-bonded Se atoms. Further computational conformational analysis of through-space coupling in these systems revealed a striking difference in the predicted ^4J(Se,Se) values depending on the conformation of the optimized structure of the molecule. For example, calculated ^4J(Se,Se) SSCCs for the four optimized structures of $Nap(SeMe)_2$ span a range between 19.5–564.8 Hz.[9]

Our own detailed conformational analyses of the related bis(tellurium) compound $Nap(TeMe)_2$ (**F**, Figure 1) revealed a similar conformational dependence of ^4J(Te,Te) through-space coupling, with a dramatic change in the magnitude of ^4J(Te,Te) SSCCs predicted upon subtle changes to the structural conformation.[11] The optimised CC*t* conformer (vide infra) is the global minimum and is predicted to have $^4J(^{125}Te,^{125}Te)$ values around 2500 Hz, whilst a conformer in the AB region is predicted to have a much lower J value (ca. 1500 Hz). A two-dimensional (2D) plot of potential energy as a function of the two C-C-Te-C_{Me} dihedral angles displayed a vast area within just 1 kcal mol^{-1} which extended from the global minimum (CC*t*) into the region classified as AB.[11] In their study of corresponding selenium derivatives, Nakanishi and colleagues concluded that this small energy difference must result in an equilibrium existing between the AB and CC*t* conformers in solution.[9] This hypothesis was supported in our own study, in which the experimentally observed J value for $Acenap(TePh)_2$ (2110 Hz; **G**, Figure 1) was found to lie intermediate between the predicted $^4J(^{125}Te,^{125}Te)$ SSCCs for the two conformers (CC*t* 2604 Hz; AB 1543 Hz).[11]

Interestingly, when the phenyl moiety was replaced by a much larger mesityl group (**H**, Figure 1), a conformational change was observed in the solid from AB to CC*t*, and despite only a 0.03 Å reduction in the Te···Te internuclear distance, this was accompanied by a significant increase in the $^4J(^{125}Te,^{125}Te)$ through-space coupling (3398 Hz).[11] This implies that the effective overlap of the interacting lone-pairs and hence the size of the SSCCs, depends not only on the internuclear distance, but also on the orientation of the lone-pairs and hence the conformation of the molecule. It therefore transpires that through-space spin–spin coupling not only probes the bonding situation between coupled nuclei, but also has the potential as an analytical tool for distinguishing between different structural conformers of a molecule.

The current study aims to develop our understanding of the conformational dependence of through-space spin–spin coupling by investigating how the electronics and sterics of substituents at Te and the architecture of the backbone, can modulate the molecular structures, intramolecular bonding interactions and NMR properties in a series of *peri*-substituted bis(tellurides). For our study we chose to compare 1,8-disubstituted naphthalenes **N** with bridged acenaphthene **A** and acenaphthylene **Ay** systems, in total synthesising 23 bis(tellurides); $Nap/Acenap/Aceyl(TeY)_2$ (Nap = naphthalene-1,8-diyl **N**; Acenap = acenaphthene-5,6-diyl **A**; Aceyl = acenaphthylene-5,6-diyl **Ay**; Y = Ph **1**; Fp **2**; Tol **3**; An-*p* **4**; An-*o* **5**; Tp **6**; Mes **7**; Tip **8**; Figure 2).

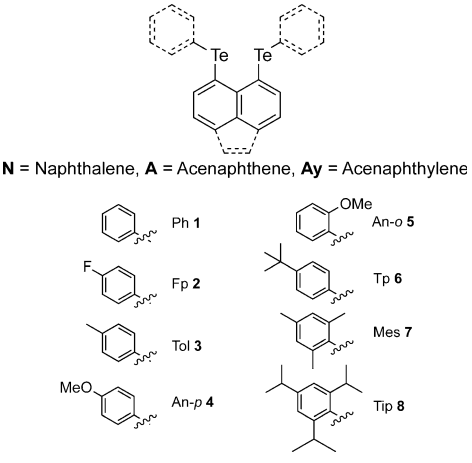

Figure 2. *Peri*-substituted bis(tellurides) **N1**–**N8**, **A1**–**A8** and **Ay1**–**Ay8**.

In these compounds the tellurium moieties are formally non-bonded, but lie at distances significantly shorter than the sum of van der Waals radii, inducing weak donor-acceptor 3-center-4-electron (3c–4e) interactions to transpire, reinforcing the through-space coupling and leading to exceptionally large $^4J(^{125}Te,^{125}Te)$ SSCCs.[11–14] Considering the shortest through-bond pathway connecting the two tellurium atoms in these systems is four bonds long, it was assumed that the contribution from through-bond coupling would be sufficiently small enough to be able to determine experimentally the conformational dependence of J_{TeTe}.[1–4,6]

Results and Discussion

Synthetic aspects

The three corresponding series of *peri*-substituted aryl tellurides were prepared from diaryl ditellurides bis(4-fluorophenyl) ditelluride (FpTeTeFp), bis(4-methylphenyl) ditelluride (TolTeTeTol), bis(4-methoxyphenyl) ditelluride (An-*p*TeTeAn-*p*), bis(2-methoxyphenyl) ditelluride (An-*o*TeTeAn-*o*), bis(4-tertbutylphenyl) ditelluride (TpTeTeTp), bis(2,4,6-trimethylphenyl) ditelluride (MesTeTeMes) and bis(2,4,6-triisopropanylphenyl) ditelluride (TipTeTeTip).[15] Naphthalenes **N2**–**N8** were prepared by following the same procedure to that previously reported for the synthesis of 1,8-bis(phenyltelluro)naphthalene **N1**;[12] under an oxygen- and a moisture-free nitrogen atmosphere, 1,8-diiodonaphthalene was independently treated with two molar equivalents of *n*-butyllithium in diethyl ether to afford the precursor 1,8-dilithionaphthalene, which when reacted with the appropriate diaryl ditelluride afforded **N2**–**N8** in moderate to good yield (yield: 65 (**N2**), 13 (**N3**), 45 (**N4**), 15 (**N5**), 51 (**N6**), 11 (**N7**), 26% (**N8**); Scheme 1).

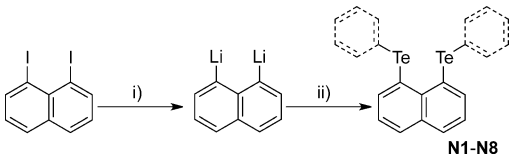

Scheme 1. Preparation of naphthalenes **N1**–**N8**: i) *n*BuLi (2.03 equiv, dropwise), Et_2O, −78 °C, 1 h; ii) RTeTeR (2 equiv), Et_2O, −78 °C, 1 h.

Acenaphthenes **A2**–**A8** were synthesised by following a slightly modified route, instead proceeding by a 5,6-dilithioacenaphthene·2 TMEDA intermediate complex, as previously described for the preparation of 5,6-bis(phenyltelluro)acenaphthene **A1** (yield: 54 (**A2**), 38 (**A3**), 53 (**A4**), 39 (**A5**), 61 (**A6**), 22 (**A7**), 54% (**A8**); Scheme 2).[13] Except for **A5**, treatment of the respective acenaphthene derivative with 2,3-dichloro-5,6-dicyano-1,4-benzoquinone (DDQ) in refluxing benzene[14] resulted in the effective dehydrogenation of the ethane backbone, affording the corresponding acenaphthylene derivative **Ay2**–**Ay4**, **Ay6**–**Ay8** (yield: 18 (**Ay2**), 23 (**Ay3**), 23 (**Ay4**), 12 (**Ay6**), 9 (**Ay7**), 14% (**Ay8**); Scheme 2).

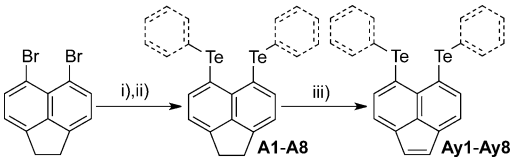

Scheme 2. Preparation of acenaphthenes **A1**–**A8** and acenaphthylenes **Ay1**–**Ay8**: i) TMEDA (2.6 equiv), *n*BuLi (2.4 equiv, dropwise), Et_2O, −10-0 °C, 1 h; ii) RTeTeR (2 equiv), Et_2O, −78 °C, 1 h; iii) DDQ (1.5 equiv), benzene, reflux, 24 h.

All compounds obtained were characterized by multinuclear magnetic resonance and IR spectroscopies and mass spectrometry, and the homogeneity of the new compounds was confirmed by microanalysis. ^{125}Te and ^{123}Te NMR spectroscopic data for all three series of bis(telluride) derivatives and their respective ditelluride starting materials is displayed in Table 1.

Table 1. ^{125}Te and ^{123}Te NMR spectroscopy data.

RTeTeR	Ph	Fp	Tol	An-*P*	An-*o*	Tp	Mes	Tip
^{125}Te NMR	428	463	432	461	176	409	202	183
^{123}Te NMR	434	464	432	461	176	410	202	183
$J(^{123}Te,^{125}Te)$	268	129	787	216	279	198	532	650
$J(^{125}Te,^{125}Te)$	323	156	949	260	336	239	642	784
	N1[12]	**N2**	**N3**	**N4**	**N5**	**N6**	**N7**	**N8**
^{125}Te NMR	620	616	608	602	515	604	397	346
^{123}Te NMR	620	616	607	602	514	605	397	346
$J(^{123}Te,^{125}Te)$	2077	2082	2145	2189	2219	2097	3191	3095
$J(^{125}Te,^{125}Te)$	2505	2511	2587	2640	2676	2529	3848	3733
	A1[13]	**A2**	**A3**	**A4**	**A5**	**A6**	**A7**	**A8**
^{125}Te NMR	586	582	574	568	482	571	363	316
^{123}Te NMR	587	580	574	568	482	572	363	316
$J(^{123}Te,^{125}Te)$	1750	1746	1780	1835	1796	1766	2818	2727
$J(^{125}Te,^{125}Te)$	2110	2106	2147	2213	2166	2130	3398	3289
	Ay1[14]	**Ay2**	**Ay3**	**Ay4**		**Ay6**	**Ay7**	**Ay8**
^{125}Te NMR	619	610	606	541		601	407	354
^{123}Te NMR	619	610	605	541		600	406	353
$J(^{123}Te,^{125}Te)$	1706	1700	1796	–		1772	2956	2958
$J(^{125}Te,^{125}Te)$	2057	2050	2166	–		2137	3565	3567

X-ray investigations

Suitable single crystals were obtained for **N2**–**N7**, **A2**–**A7** and **Ay2** by diffusion of hexane into a saturated solution of the compound in dichloromethane. Crystals for **Ay3**, **Ay4**, **Ay7** and **Ay8** were obtained by evaporation of a dichloromethane solution of the product, for **A8** by evaporation of a hexane solution and similarly for **Ay5** from a chloroform solution. All compounds contain only one molecule in the asymmetric unit. Selected interatomic bond lengths and angles are listed in Tables S1–S3 (Supporting Information) and further crystallographic information can be found in the Supporting Information.

The molecular structures of *peri*-substituted systems are regularly categorised using the classification system devised by Nakanishi et al.[16] and Nagy et al.,[17] whereby the conformation of the *peri*-atom-substituent bond (with respect to the mean plane of the organic backbone) is described as either perpendicular (A or axial), coplanar (B or equatorial) or intermediate

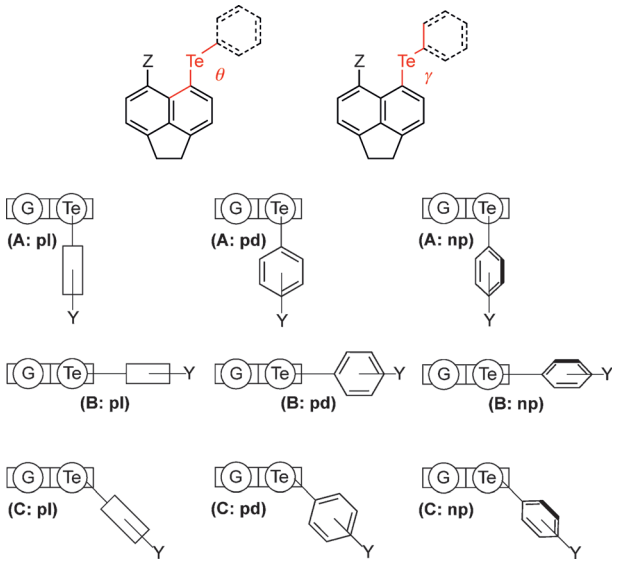

Figure 3. The absolute conformation of aromatic rings is calculated from torsion angles θ (defining rotation around the Te–$C_{Nap'}$ bond) and classified by types **A** (axial, perpendicular), **B** (equatorial, planar) or **C** (twist).[16,17]

between these two scenarios (C or twist; Figure 3). A double substitution can subsequently result in either a *cis* (*c*) or *trans* (*t*) arrangement of the two substituent bonds relative to the naphthalene plane. The absolute conformation of the Te(aryl) groups is calculated from torsion angles θ, which defines the degree of rotation around each Te–$C_{Nap'}$ bond (Table 2, Figure 3).

In the solid, all bis(tellurides) investigated as part of this study adopt either a CC*t* conformation, similar to what is found for **N1**[11,12] and **A7**,[11] or an AB conformation comparable to that observed for **A1**[11,13] (Figure 3–5, Table 2). Compound **A8** (Tip) is the one anomaly in the series, adopting a slightly modified BC*c* type arrangement in the solid (Figure 5, Table 2). The structural variation observed in the solid for this family of compounds is consistent with the conformational analysis carried out on $Nap(TeMe)_2$[11] and related selenium derivatives,[9] which revealed that AB and CC*t*-type conformers are the most stable and very close in energy (within 1 kcal mol^{-1}), and as such can thus be controlled by subtle changes to the steric and electronic properties of the *peri*-substituents.

Nevertheless, certain trends are observed across the three series, with, for example, mesityl (Mes), *para*-anisole (An-*p*) and toluene (Tol) derivatives invariably adopting CC*t* type arrangements (Figure 4 and 5) and *ortho*-anisole (An-*o*) and *tert*-butylphenyl (Tp) analogues favouring AB configurations (Figure 4 and 5). Whilst this suggests the nature of the Te(aryl) moiety rather than the type of organic backbone dictates the final molecular conformation in these compounds, substituent size is certainly not the only factor involved. The steric bulk of the aryl functionalities can be quantified by measuring the Te(aryl) group cone angle, with the steric parameter (θ) defined as the apex angle that extends from the hydrogen atoms at the extreme edges of the cone to the central Te atom at the vertex.[18] Using this method, the steric bulk of the aryl groups is shown to increase in the order 81 (Ph, Fp, Tol, An-*p*, Tp) < 105 (An-*o*) < 123 (Mes) < 134° (Tip), which helps to illustrate the lack of correlation between the size of the substituents bound to Te and the conformation adopted in the solid. For instance, Te(Tol) (**3**) and Te(An-*p*) (**4**) derivatives favour CC*t* conformations, contrasting with the AB conformation imposed by the similarly sized Te(Tp) (**6**) moiety. It is worth noting, however, that derivatives substituted with larger moieties, such as Te(Mes) (**7**) and Te(Tip) (**8**), prefer to adopt CC*t* conformations in the solid, a result which became more apparent during the analysis of the solution-state structures (vide infra).

The double substitution of increasingly large atoms or groups on a *peri*-backbone invariably causes greater repulsion and an increase in steric pressure within the bay region due to the overlap of closely aligned orbitals.[19–21] With this in mind, it would be expected that as larger Te(aryl) groups, such as Te(Mes) (**7**) and Te(Tip) (**8**), are located at the proximal *peri*-positions greater deformation of the carbon framework would be required to accommodate the extra bulk,[19–21] as discovered recently in a series of analogous tellurium–selenium acenaphthenes;[18] however, no apparent correlation is found between the steric bulk of the Te(aryl) functionality (steric parameter, θ) and the degree of molecular distortion occurring within the organic framework. Non-bonded Te···Te *peri*-separations for the naphthalene series are within just 0.08 Å and span a range from 3.2623(7) Å in **N7** (Te(Mes); $\theta = 120°$) to 3.3436(6) Å in **N6**

Table 2. Torsion angles [°] categorising the aromatic-ring conformations in **N1**–**N8**, **A1**–**A8** and **Ay1**–**Ay8**.

Comp.	C(10)-C(1)-Te(1)-C(11)	C(10)-C(9)-Te(2)-C(18)	
N1	θ_1 −124.79(1) twist[c]	θ_2 −132.46(1) twist	CC*t*
N2	θ_1 −145.4(4) twist	θ_2 −146.2(4) twist	CC*t*
N3	θ_1 −148.5(4) twist	θ_2 −149.4(4) twist	CC*t*
N4	θ_1 −125.1(8) twist	θ_2 −134.8(8) twist	CC*t*
N5	θ_1 177.2(6) equatorial[b]	θ_2 −110.1(6) axial	AB
N6	θ_1 −77.0(3) axial[a]	θ_2 −169.3(3) equatorial	AB
N7	θ_1 138.8(4) twist	θ_2 −142.8(4) twist	CC*t*
Comp.	**C(10)-C(1)-Te(1)-C(13)**	**C(10)-C(9)-Te(2)-C(19)**	
A1	θ_1 166.60(1) equatorial	θ_2 79.56(1) axial	AB
A2	θ_1 −167.3(6) equatorial	θ_2 −80.3(5) axial	AB
A3	θ_1 −153.3(5) twist	θ_2 −142.0(5) twist	CC*t*
A4	θ_1 153.3(9) twist	θ_2 144.2(9) twist	CC*t*
A5	θ_1 −165.8(4) equatorial	θ_2 −84.4(4) axial	AB
A6	θ_1 169.3(6) equatorial	θ_2 72.5(8) axial	AB
A7	θ_1 −152.1(6) twist	θ_2 −136.4(6) twist	CC*t*
A8	θ_1 142.6(4) twist	θ_2 −169.4(4) equatorial	BC*c*
Comp.	**C(10)-C(1)-Te(1)-C(13)**	**C(10)-C(9)-Te(2)-C(19)**	
Ay1	θ_1 78.8(7) axial	θ_2 166.2(7) equatorial	AB
Ay2	θ_1 165.4(3) equatorial	θ_2 90.5(3) axial	AB
Ay3	θ_1 152.2(9) twist	θ_2 145.7(9) twist	CC*t*
Ay4	θ_1 −142.6(7) twist	θ_2 −152.0(7) twist	CC*t*
Ay6	θ_1 68.2(17) axial	θ_2 −164.5(19) equatorial	AB
Ay7	θ_1 145.3(7) twist	θ_2 152.9(7) twist	CC*t*
Ay8	θ_1 133.1(3) twist	θ_2 133.1(3) twist	CC*t*

[a] axial: perpendicular to C(ar)-Te-C(ar) plane. [b] equatorial: coplanar with C(ar)-Te-C(ar) plane. [c] twist: intermediate between axial and equatorial.

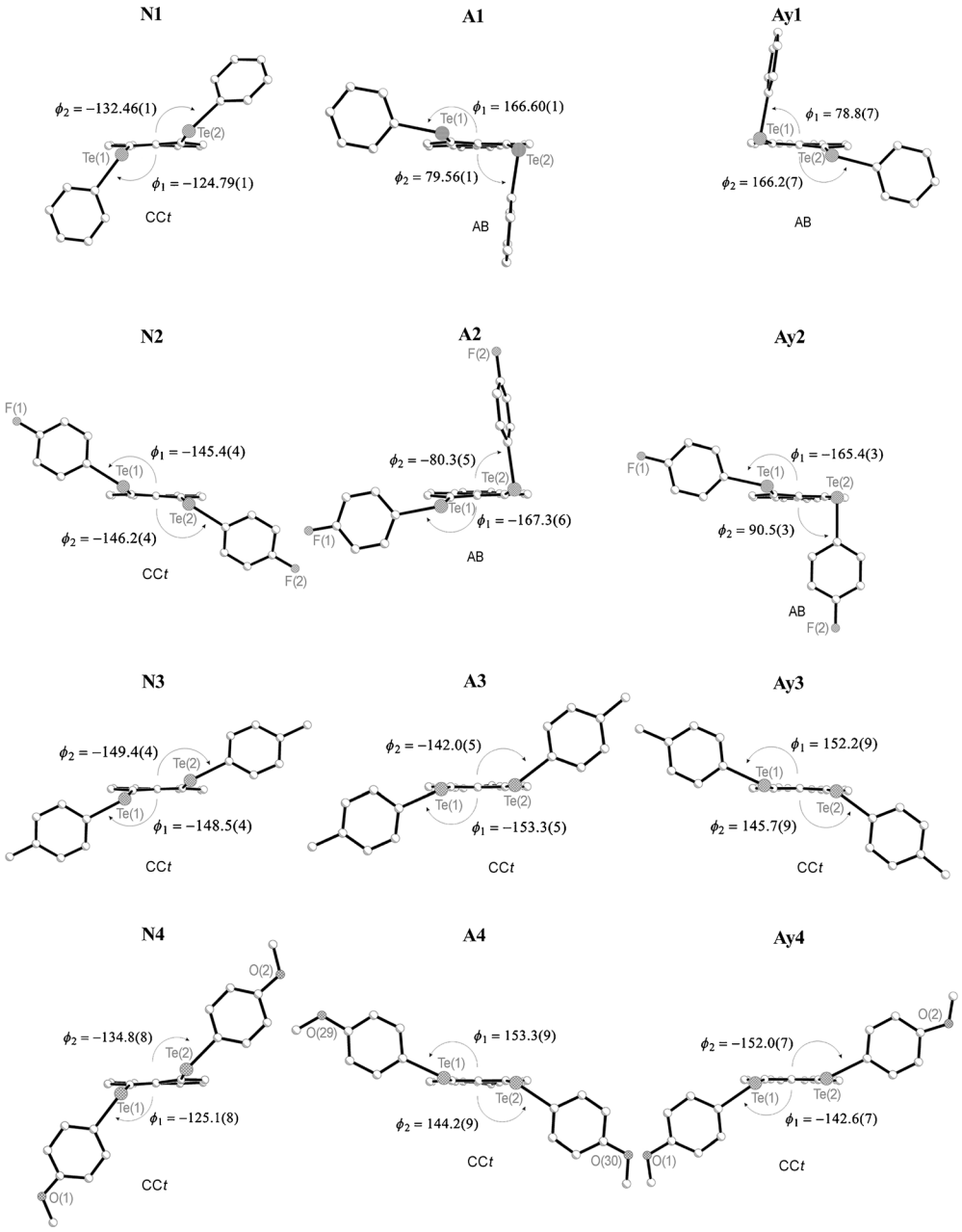

Figure 4. Molecular conformations of Te(Ph) (**1**), Te(Fp) (**2**), Te(Tol) (**3**) and Te(An-*p*) (**4**) derivatives substituted on naphthalene (**N**), acenaphthene (**A**) and acenaphthylene (**Ay**) organic backbones, showing the orientation of the substituents bound to Te. All compounds adopt either a CC*t* or AB configuration in the solid.

(Te(Tp); $\theta = 81°$). As expected,[13,14] marginally longer Te···Te *peri*-distances are observed in corresponding acenaphthene (3.3204(15) Å **A4** Te(An-*p*)—3.933(13) Å **A6** Te(Tp)) and acenaphthylene (3.3337(12) Å **Ay4** Te(An-*p*)—3.437(3) Å **Ay6** Te(Tp)) derivatives due to the additional constraints of the bridging ethane/ethene organic linkers that naturally widen the bay region. Nevertheless, little variation is observed in d_{TeTe} for different molecular conformations or Te(aryl) functionalities, with separations differing by only 0.07 and 0.10 Å in the two series, respectively.

The plot in Figure 6 displays the relationship between the nonbonded Te···Te distance and the form of the Te(aryl) group for the three series of bis(tellurides) and whilst d_{TeTe} values only vary by 0.17 Å, the effect each organic backbone has on the Te···Te interaction is clearly illustrated. Similar trends are observed across all three series, with Te(Mes) and Te(An-*p*) derivatives providing the smallest Te···Te separations and maximum d_{TeTe} values observed for Te(Tp) analogues. Interestingly, CC*t* conformers constantly exhibit shorter Te···Te distances than AB variants. This is consistent with the findings from previous studies of related chalcogen-substituted compounds[12–14] and the computational conformational analysis previously carried out on $Nap(TeMe)_2$.[11]

For instance, the two-dimensional (2D) Ramachandran-type plot in Figure 7 represents the nonbonded Te···Te *peri*-distance in $Nap(TeMe)_2$ as a function of the two C9-C-Te-C(Me) dihedral angles. Here a structure with CC*t* conformation is computed to have a relatively short *peri*-separation of around 3.3 Å, with structures in the AB region predicted to have notably longer Te···Te distances up to 3.5 Å.[11] Whilst the computed values from the computational analysis of $Nap(TeMe)_2$ are marginally overestimated with respect to experimental values obtained for the three series, the predicted tendency is confirmed qualitatively (Figure 8).

Despite the apparent conformational dependence of *d*(Te,Te), nonbonded Te···Te *peri*-distances for all bis(tellurides) of this study are 17–21% shorter than twice the van der Waals radii of Te (4.12 Å).[10] In all cases, the close proximity of the tellurium atoms and the orientation of the molecule provides the correct geometry to promote delocalization of a tellurium lone pair to an antibonding $\sigma^*(Te–C_{Ar})$ orbital to form an energy-lowering, donor–acceptor three-center–four-electron (3c–4e)-type interaction. Such nonbonded interactions provide a convenient pathway through which scalar *J* spin couplings can operate, and result in exceptionally large through-space $J(^{125}Te,^{125}Te)$ SSCCs.

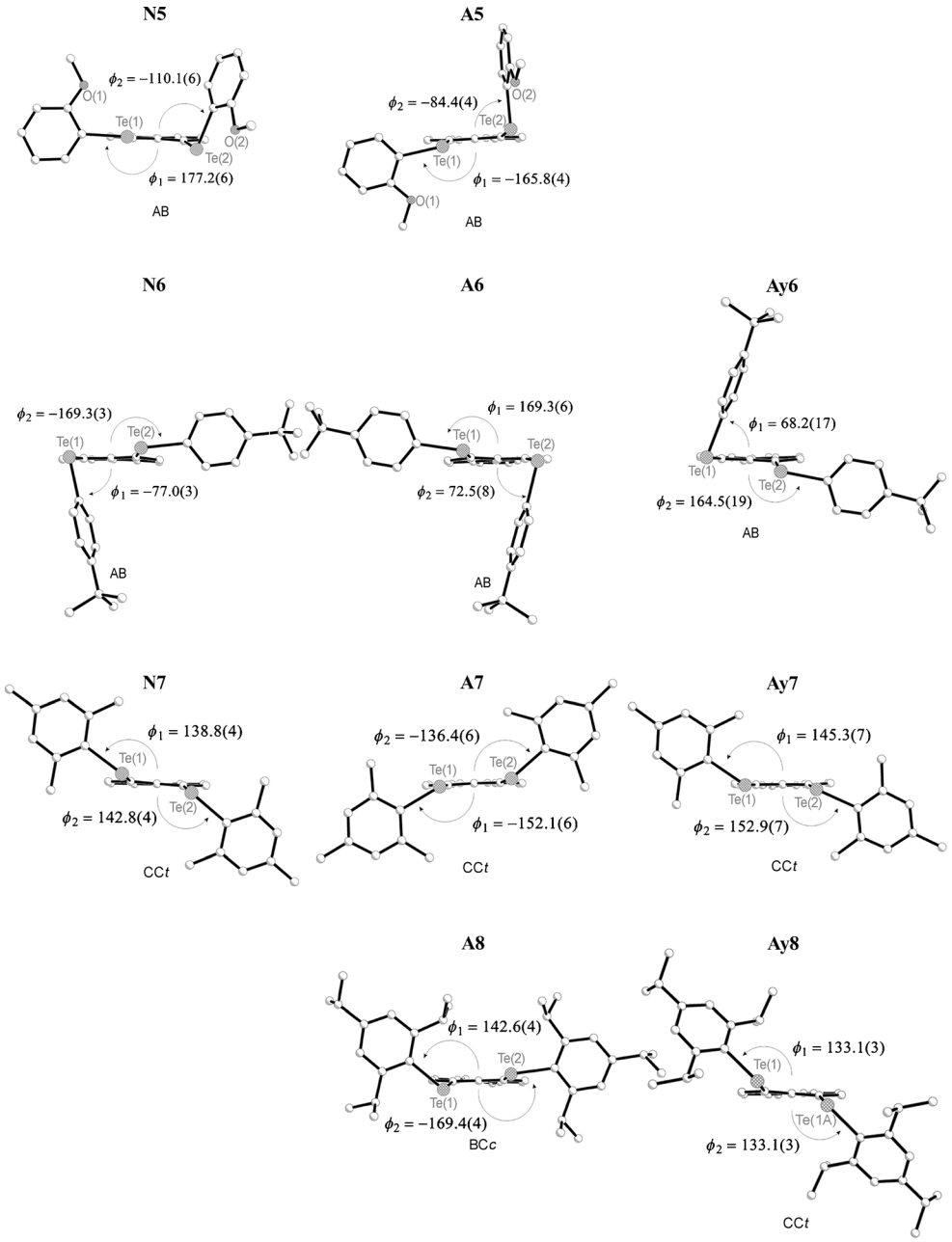

Figure 5. Molecular conformations of Te(An-*o*) (**5**), Te(Tp) (**6**), Te(Mes) (**7**) and Te(Tip) (**8**) derivatives substituted on naphthalene (**N**), acenaphthene (**A**) and acenaphthylene (**Ay**) organic backbones, showing the orientation of the substituents bound to Te. All compounds except **A8** adopt either a CC*t* or AB configuration in the solid.

between the two values arising from subtle differences in the molecular dynamics of the two compounds in solution.[11] In the solid, **N1**[11,12] and **A1**[11,13] adopt conformations in the CC*t* and AB regions, but in solution both compounds appear to be rather fluxional due to the negligible energy difference predicted between these two types of conformers.[11] Considering such a dramatic variation in through-space $J(^{125}Te,^{125}Te)$ spin–spin coupling is achieved with only a minor change to the conformation (~1000 Hz between CC*t* and AB),[11] the relatively small deviation observed in the *J* values for **N1** and **A1** is thus likely to arise from subtle shifts in conformer equilibrium, rather than reflecting the conformation of each compound in the solid. By contrast, the truly massive $J(^{125}Te,^{125}Te)$ value of 3398 Hz obtained for the mesityl derivative **A8**,[11] indicates a considerable shift in the conformer populations in solution towards a CC*t* type arrangement, now consistent with the structure found in the solid.[11]

The plot in Figure 9 shows the relationship between $J(^{125}Te,^{125}Te)$ and the aryl moiety for all three series, again illustrating the effect each backbone has on the coupling value. Interestingly the naphthalene series exhibits notably larger through-space coupling compared to the values obtained for corresponding acenaphthene and acenaphthylene analogues, which is consistent with the shorter Te···Te *peri*-distances naturally found in naphthalene derivatives (Figure 6), and thus shows a form of distance dependence on J_{TeTe}.

Solution NMR spectroscopic studies

For symmetrical systems, such as ditellurides or the series of bis(tellurides) of this study, the magnetic equivalence of two Te nuclei impedes direct observation of $J(^{125}Te,^{125}Te)$ coupling in solution-state ^{125}Te NMR spectra. Nevertheless, $J(^{125}Te,^{125}Te)$ values can be converted from experimentally obtained $J(^{123}Te,^{125}Te)$ coupling, detected as satellites in the ^{123}Te NMR spectra. Using this technique, exceptionally large $J(^{125}Te,^{125}Te)$ SSCCs have previously been obtained for phenyl derivatives **N1** (2505 Hz) and **A1** (2110 Hz), with the large discrimination

Within all three series a striking variation is observed in through-space $J(^{125}Te,^{125}Te)$ spin–spin coupling (2050-3848 Hz) depending on the nature of the Te(aryl) functionality employed. For compounds substituted with smaller Te(aryl) groups (Ph, Fp, Tol, An-*p*, An-*o*, Tp; $\theta = 81–105^\circ$), $J(^{125}Te,^{125}Te)$ values of 2505–2676 (**N1**–**N6**), 2106–2213 (**A1**–**A6**) and 2050–2166 Hz (**Ay1**–**Ay6**) are found, whilst bulkier Mes and Tip derivatives ($\theta = 123–134^\circ$) afford substantially higher *J* values (3289–3848 Hz). Because the *J* coupling changes so dramatical-

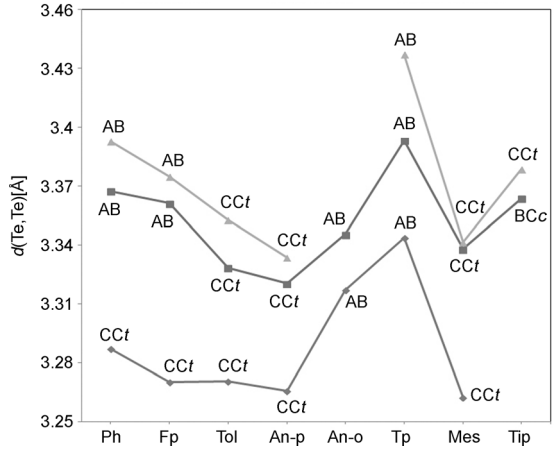

Figure 6. Plot showing the variation in the nonbonded Te···Te *peri*'distances for the three series of analogous bis(tellurides). ▲: acenaphthylene; ■: acenaphthalene; ●: naphthalene.

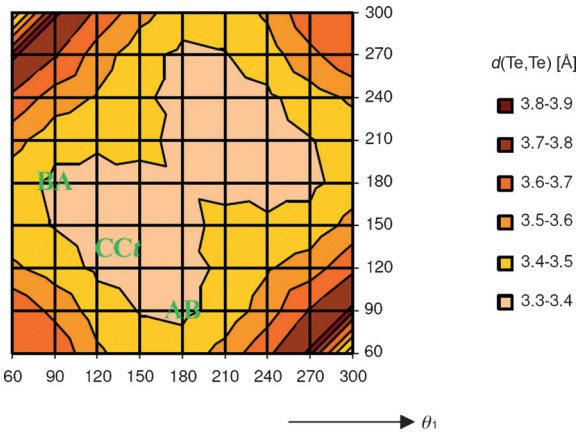

Figure 7. Non-bonded Te···Te distances (B3LYP/SDD/6-31G* level) in Nap(-TeMe)$_2$ as a function of the conformation, as defined by the two C9-C-Te-C(Me) dihedral angles (θ).[11]

ly with conformation,[11] the extremely small range of SSCCs found between Ph, Fp, Tol, An-*p*, An-*o* and Tp derivatives in all three series (ΔJ_{TeTe} **N1**–**N6** 171 Hz; ΔJ_{TeTe} **A1**–**A6** 107 Hz; ΔJ_{TeTe} **Ay1**–**Ay6** 116 Hz) indicates the conformational similarity of the structures in solution. This is in stark contrast to their behaviour in the solid-state (vide supra), in which a mixture of AB and CC*t* conformations are obtained, but it is consistent with the theory that an equilibrium must exist between AB and CC*t* conformers in solution due to the small difference in their potential energies.[10,11] In spite of this, an excellent correlation is observed between the $\delta(^{125}Te)$ values for the naphthalene series and those of their acenaphthene analogues (Figure S3, Supporting Information), which indicates that in solution the structural conformation around the two Te atoms in related compounds must be very close.[16 g]

Considering the $J(^{125}Te,^{125}Te)$ values for the less bulky derivatives are significantly smaller than for Mes and Tip analogues (by 1057–1399 Hz), it is assumed that the conformer equilibrium is shifted towards greater populations of AB conformers, and thus the *J* values obtained from solution-state NMR spectra may not necessarily reflect the structural conformations found in the solid for these compounds. Conversely, the exceptionally large $J(^{125}Te,^{125}Te)$ values obtained for the Mes and Tip

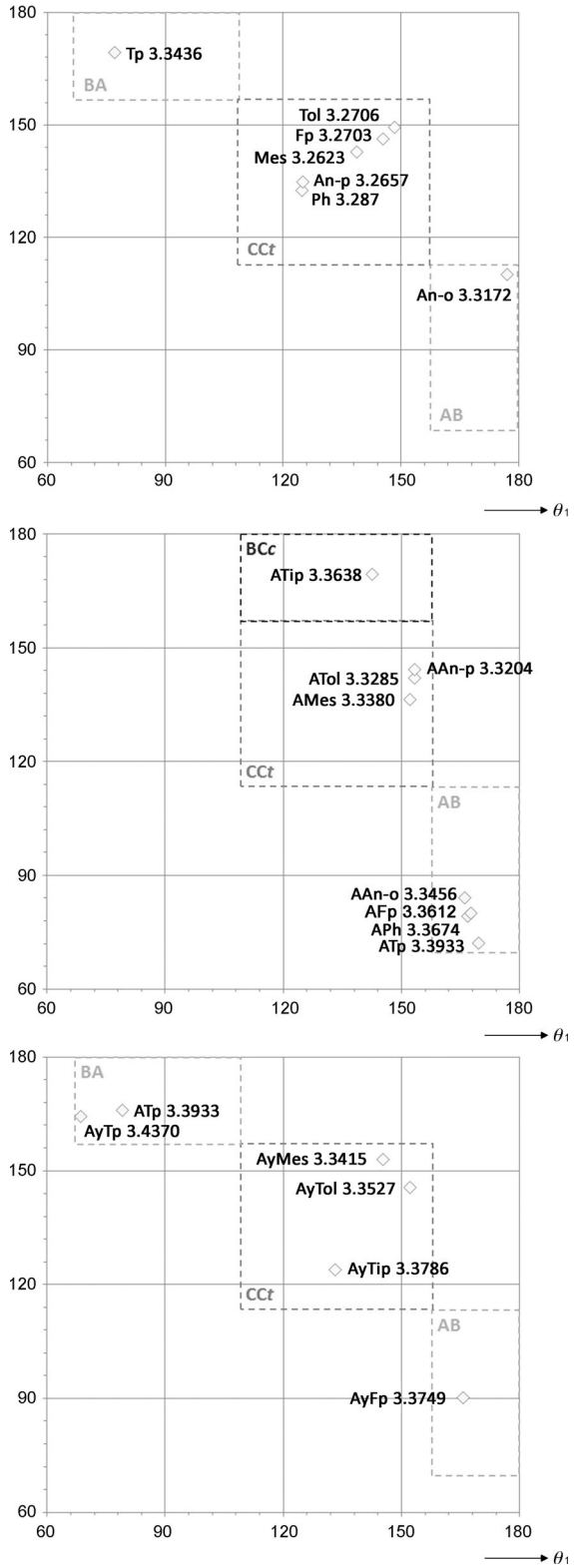

Figure 8. Experimentally obtained Te···Te *peri*-distances in naphthalene (top), acenaphthene (middle) and acenaphthylene (bottom) derivatives as a function of the two C9-C-Te-C(R) dihedral angles.

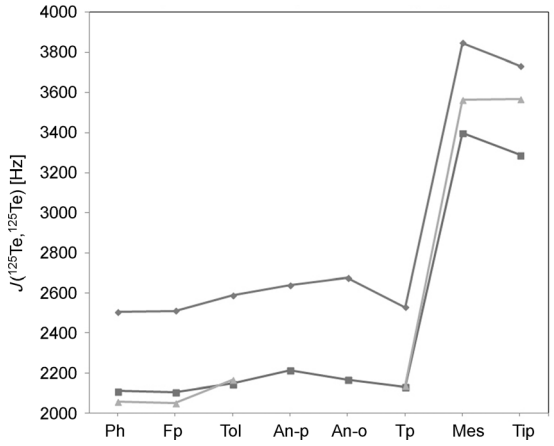

Figure 9. Plot showing the dramatic change in $J(^{125}Te,^{125}Te)$ for different members of all three series of bis(tellurides).

compounds are consistent with a CC*t* conformation in solution,[11] in agreement with the molecular structures determined by X-ray crystallography.

To the best of our knowledge, the value of 3848 Hz obtained for **N7** is the largest SSCC observed to date between formally non-bonded Te atoms. In fact $J(^{125}Te,^{125}Te)$ values with a mean greater than 2000 Hz, as observed for all members of this study, are quite considerable for formal ^4J coupling. For comparison, ^1J through-bond SSCCs of only 156–949 Hz were obtained for the parent ditellurides (RTeTeR; R = Ph, Fp, Tol, An-*p*, An-*o*, Tp, Mes, Tip; Table 1),

Solid-state NMR spectroscopy

The crystal structure of compound **Ay8** contains one crystallographically distinct molecule per asymmetric unit, but the two tellurium atoms within this molecule are crystallography inequivalent, and so it is possible to estimate the through-space *J* coupling between the two *peri* atoms using solid-state NMR spectroscopy. However, the presence of a significant ^{125}Te chemical shift anisotropy (CSA) results in a significant number of spinning sidebands, hindering the accurate analysis of both shielding and coupling tensors.

The splittings observed in the isotropic peaks (at 354 and 316 ppm) although not completely resolved, can be estimated as between 3600 and 4000 Hz, although a more detailed analysis would be required to extract the full tensorial information on both interactions. As an example, the ^{125}Te spectra of compound **Ay8** (at 9.4 T and 14.1 T) are shown in Figure 10.

DFT calculations

To probe how well the findings from X-ray structural analysis and solution-state NMR studies could be reproduced and rationalised computationally, and specifically to assess the extent of conformational dependence of through-space $J(^{125}Te,^{125}Te)$ spin–spin coupling in these *peri*-substituted bis(telluride) systems, DFT calculations were performed for the phenyl (**N1**, **A1**, **Ay1**), tolyl (**N3**, **A3**, **Ay3**), *para*-anisyl (**N4**, **A4**, **Ay4**) and mesityl (**N7**, **A7**, **Ay7**) derivatives of this study (Table 3).

First, atomic coordinates obtained from X-ray crystallography were optimized at the B3LYP/SDD/6-31G* level, which was chosen for compatibility with our previous calculations on related bis(chalcogen) species.[11–14] At this level all four naphthalenes (**N1**, **N3**, **N4** and **N7**) and the two additional mesityl derivatives (**A7** and **Ay7**) optimise to a CC*t* conformation in which both dihedral angles (θ) align close to 140°, corresponding to the structure found in the solid in each case. In contrast, both AB and CC*t* minima are found for the remaining acenaphthene (**A1**, **A3**, **A4**) and acenaphthylene (**Ay1**, **Ay3**, **Ay4**) derivatives.

In all cases the computed Te···Te nonbonded *peri*-distance is notably overestimated compared to that observed in the solid (by up to 0.09 Å); however, this is a common DFT problem and a good linear correlation is found between the computed distances and those obtained experimentally from X-ray data (Fig-

Table 3. Selected bond distances (Å) from X-ray crystallography and B3LYP optimisations (in brackets: Wiberg bond indices at the B3LYP level) and $J(^{125}Te,^{125}Te)$ couplings from solution-state NMR studies and ZORA-SO/BP//B3LYP computations.

	N1[12]	**N3**	**N4**	**N7**
Aryl Group	Ph	Tol	An-*p*	Mes
Exptl. Te···Te [Conf.]	3.287(1) [CC*t*]	3.2706(8) [CC*t*]	3.2657(15) [CC*t*]	3.2623(7) [CC*t*]
Calcd Te···Te [WBI] AB	n/a	n/a	n/a	n/a
CC*t*	3.341 [0.15]	3.351 [0.14]	3.355 [0.14]	3.356 [0.14]
Exptl. $J(^{125}Te,^{125}Te)$	2505	2587	2640	3848
Calcd $J(^{125}Te,^{125}Te)$ CC*t*	2779	3078	3191	3153
	A1[13]	**A3**	**A4**	**A7**
Aryl Group	Ph	Tol	An-*p*	Mes
Exptl. Te···Te [Conf.]	3.3674(19) [AB]	3.3285(7) [CC*t*]	3.3204(15) [CC*t*]	3.3380(11) [CC*t*]
Calcd Te···Te [WBI] AB	3.438 [0.13]	3.440 [0.13]	3.448 [0.13]	n/a
CC*t*	3.412 [0.13]	3.414 [0.13]	3.415 [0.13]	3.422 [0.12]
Exptl. $J(^{125}Te,^{125}Te)$	2110	2147	2213	3398
Calcd $J(^{125}Te,^{125}Te)$ AB	1543	1591	1375	n/a
CC*t*	2604	2699	2842	2738
	Ay1[14]	**Ay3**	**Ay4**	**Ay7**
Aryl Group	Ph	Tol	An-*p*	Mes
Exptl. Te···Te [Conf.]	3.393(3) [AB]	3.3527(14) [CC*t*]	3.3337(12) [CC*t*]	3.3415(11) [CC*t*]
Calcd Te···Te [WBI] AB	3.451 [0.13]	3.453 [0.13]	3.466 [0.12]	n/a
CC*t*	3.425 [0.12]	3.423 [0.12]	3.427 [0.12]	3.432 [0.11]
Exptl. $J(^{125}Te,^{125}Te)$	2057	2166	–	3565
Calcd. $J(^{125}Te,^{125}Te)$ AB	1465	1438	1317	n/a
CC*t*	2798	2879	2978	2918

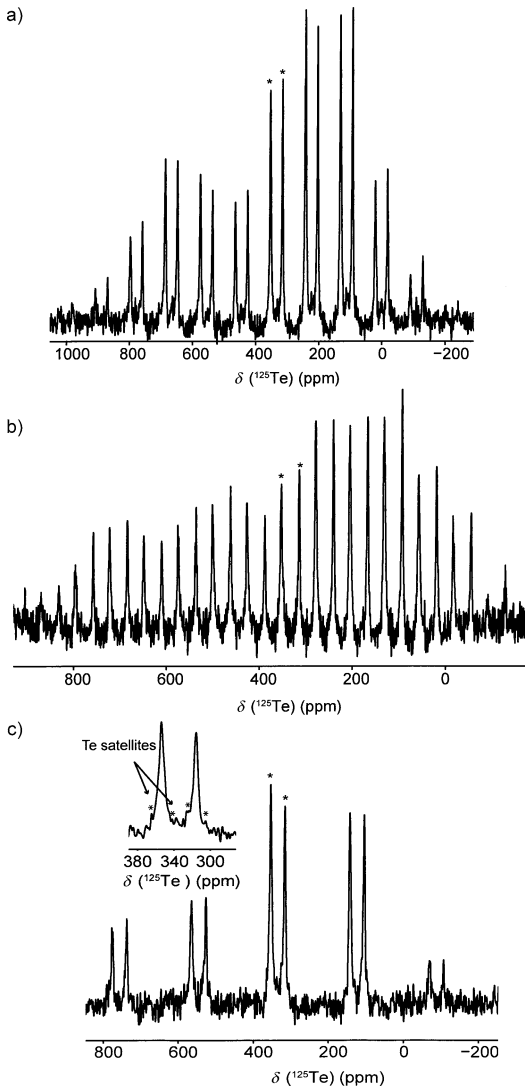

Figure 10. ^{125}Te solid-state (B_0 = 9.4 T) NMR spectra of **Ay8**, recorded using a) MAS rates of 14 kHz. b) ^{125}Te solid-state (B_0 = 14.1 T); MAS rates of 14 kHz. c) using MAS rates of 40 kHz (B_0 = 14.1 T).

ure S2, Supporting Information). Consistent with the findings from our previous conformational analysis of Nap(TeMe)$_2$, the trend towards longer Te···Te separations on going from CC*t* to AB conformations is captured well in the computations for acenaphthenes (**A1**, **A3**, **A4**) and acenaphthylenes (**Ay1**, **Ay3**, **Ay4**), with distances increasing by approximately 0.04 Å. Nevertheless, the extent of covalent bonding between the two Te centres is predicted to be fairly similar throughout the three series of compounds, with calculated Wiberg Bond Indices (WBI)[22] decreasing only marginally from 0.15–0.14 for the set of naphthalene compounds (**N1**, **N3**, **N4**, **N7**) to 0.13–0.11 for their acenaphthene and acenaphthylene analogues.

Next, computed (ZORA-SO/BP//B3LYP level) J(^{125}Te,^{125}Te) SSCCs were obtained for all twelve compounds, including predicted J values for AB and CC*t* variants in which both conformers are found. Figure 11 displays a plot of the computed versus the experimental data, with three distinct regions clearly defined.

The first is made up by the three points on the right-hand side representing the bulky mesityl derivatives **N7**, **A7** and **Ay7**, and whilst the observed couplings are significantly underestimated (systematically by ca. 650 Hz), the computed trend fits well to the experimentally obtained J values. Theoretical J values are, amongst other variables, rather sensitive to the level of geometry optimization employed in the NMR calculation, and in line with previous results,[11] going from B3LYP- to PBE0-optimised geometries brings down the error to approximately 400 Hz (results not shown). Nevertheless, the computational results support the findings from X-ray data and solution-state NMR spectroscopy, which indicates that these three bulky species are essentially locked in the CC*t* conformation.

The second region is comprised of the remaining naphthalene species **N1**, **N3** and **N4**. Similar to the three mesityl derivatives, only a single minimum is found for each compound in the region classed as CC*t* (corresponding to the structure found in the solid) and correspondingly, computed J values are naturally relatively large. In fact the couplings are significantly overestimated with respect to experiment indicating these systems are quite dynamic and explore a significant region in phase space extending toward AB conformers with their lower couplings.[11] The J coupling has been traced back to the overlap between the "sp^2"-type lone pairs on the Te atoms.[11] Apparently this overlap is somewhat reduced in the AB conformers compared to that in the CCt forms (see Figure S1 in the Supporting Information).

Finally the third region formed by the clusters on the left corresponds to the remaining acenaphthene and acenaphthylene species substituted by Te(Ph), Te(Tol) and Te(An-*p*) groups. Here we can find both AB and CC*t* minima, and the observed couplings are "bracketed" by the values computed for CC*t*, which are overestimated, and for AB, which are underestimated. Neither set shows any correlation with experiment, nor does the 50:50 average between the two (* in Figure 11). These species are thus predicted to be even "more dynamic" than the second group and explore an even larger region in phase space. The actual coupling is not only governed by the "intrinsic" substituent effects, but will also depend on the dynamic averaging. On going from, for example, Ph to Tol to An-*p* the aryl rings not only become more electron rich, their moment of inertia is bound to change as well (i.e. the angular momentum about the *peri*-Te bonds), and that may influence the dynamics. Averaging the chemical shifts over long enough trajectories from molecular dynamics simulations would be required to address this question more quantitatively, but this would be a formidable computational effort exceeding the scope of the present paper.

Conclusions

A combination of X-ray crystallography, NMR spectroscopy and DFT calculations has been used to investigate the conformational dependence of through-space J(^{125}Te,^{125}Te) spin–spin coupling in three analogous series of *peri*-substituted bis(tellurides); Nap/Acenap/Aceyl(TeY)$_2$ (Nap = naphthalene-1,8-diyl **N**; Acenap = acenaphthene-5,6-diyl **A**; Aceyl = acenaphthylene-

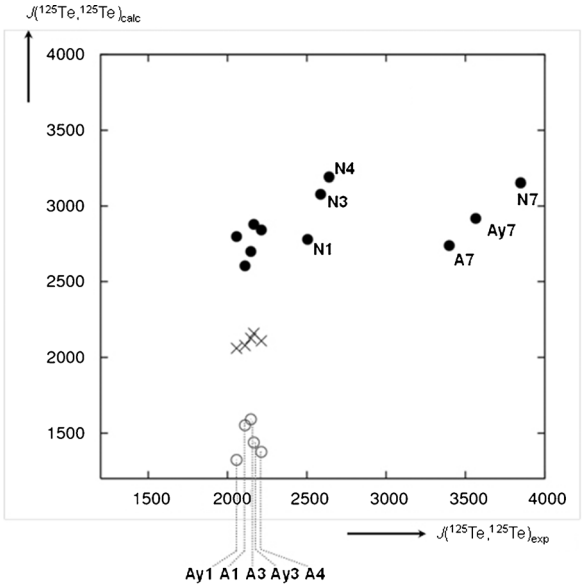

Figure 11. Plot of optimized (ZORA-SO/BP//B3LYP) vs. observed (solution-state NMR spectra) $J(^{125}Te,^{125}Te)$ SSCCs. ○: AB; ●: CCt; x: av.[a] All spectra run in $CDCl_3$; δ (ppm), J (Hz).

5,6-diyl **Ay**; Y = Ph **1**; Fp **2**; Tol **3**; An-*p* **4**; An-*o* **5**; Tp **6**; Mes **7**; Tip **8**).

In the solid, all compounds adopt AB or CC*t* conformations, with larger mesityl and triisopropyl derivatives invariably favouring the CC*t* variant. The one anomaly in the series is **A8** which adopts a BC*c* arrangement, but DFT calculations confirm this optimizes to a CC*t* conformation and thus the structure observed is likely to result from intermolecular interactions or packing forces.

Exceptionally large through-space $J(^{125}Te,^{125}Te)$ spin–spin couplings (3289–3848 Hz) are observed experimentally for derivatives substituted with bulky mesityl and triisopropyl groups, consistent with the structure found in the solid and indicating these species are permanently locked in a CC*t*-type conformation. This is supported by DFT calculations with the computed trend fitting well to the experimentally obtained J values and a single minima found for each compound (CC*t*).

In contrast, compounds substituted by smaller Te(aryl) groups display much lower J values (2050–2676 Hz), which suggests in solution these species are rather fluxional and explore a significant region in phase space extending toward AB conformers with their lower couplings. Computed J values for naphthalenes **N1**, **N3** and **N4** are significantly overestimated, whilst the observed couplings for the remaining set of compounds, for which both AB and CCt minima are found, are "bracketed" by the values computed for CC*t* (too high) and AB (too low). This is consistent with previous findings that an equilibrium must exist between AB and CC*t* conformers in solution due to the small difference in their potential energies.[10,11]

Through-space spin–spin coupling can thus act not only as a sensitive probe for investigating the underlying bonding situation between two interacting NMR spectroscopic active nuclei, but can also be used as a tool for determining molecular conformation, the dynamics of species and thus their conformer populations in solution.

Experimental Section

All experiments were carried out under an oxygen- and moisture-free nitrogen atmosphere using standard Schlenk techniques and glassware. Reagents were obtained from commercial sources and used as received. Dry solvents were collected from a MBraun solvent system. Elemental analyses were performed by Stephen Boyer at the London Metropolitan University. IR spectra were recorded as KBr discs in the range 4000–300 cm^{-1} on a Perkin–Elmer System 2000 Fourier transform spectrometer. ^1H, ^{13}C and ^{19}F NMR spectra were recorded on a Bruker AVANCE 300 MHz spectrometer with δ(H) and δ(C) referenced to external tetramethylsilane and δ(F) referenced to external trichlorofluoromethane. ^{123}Te and ^{125}Te NMR spectra were recorded on a Jeol GSX 270 MHz spectrometer with δ(Te) referenced to Me_2Te, with a secondary reference for δ(Te) to diphenyl ditelluride (δ(Te) = 428 ppm). $J(^{125}Te,\ ^{125}Te)$ values are obtained by multiplying the experimentally obtained $J(^{123}Te,\ ^{125}Te)$ values by 1.206, the ratio of the gyromagnetic ratios for ^{125}Te (-8.51×107 rad T-1 S-1)[3] and ^{123}Te (-7.06×107 rad T-1 S-1).[3] Assignments of ^{13}C and ^1H NMR spectra were made with the help of H-H COSY and HSQC experiments. All measurements were performed at 25 °C. All values reported for NMR spectroscopy are in parts per million (ppm). Coupling constants (J) are given in Hertz (Hz). Mass spectrometry was performed by the University of St Andrews Mass Spectrometry Service. Electrospray Mass Spectrometry (ESMS) was carried out on a Micromass LCT orthogonal accelerator time of flight mass spectrometer. 1,8-diiodonaphthalene[23] and 5,6-dibromoacenaphthene[24] were prepared following standard literature procedures.

Diaryl ditellurides: (ArTeTeAr)

Diphenyl ditelluride was obtained from commercial sources and used as received. Bis(4-methylphenyl) ditelluride (TolTeTeTol), bis(4-methoxyphenyl) ditelluride (An-*p*TeTeAn-*p*), bis(2-methoxyphenyl) ditelluride (An-*o*TeTeAn-*o*), bis(4-tertbutylphenyl) ditelluride (TpTeTeTp), bis(2,4,6-trimethylphenyl) ditelluride (MesTeTeMes) and bis(2,4,6-triisopropanylphenyl) ditelluride (TipTeTeTip) were synthesised from the respective aryl bromides following the procedure outlined by Ando and co-workers.[14]

PhTeTePh: ^{125}Te NMR (85.2 MHz, $CDCl_3$, 25 °C, PhTeTePh): δ = 427.6 ppm (s); ^{123}Te NMR (70.7 MHz, $CDCl_3$, 25 °C, PhTeTePh): δ = 434.1 ppm (s, $^1J(^{123}Te,^{125}Te)$ = 268 Hz).

TolTeTeTol: ^{125}Te NMR (85.2 MHz, $CDCl_3$, 25 °C, PhTeTePh): δ = 432.8 ppm (s); ^{123}Te NMR (70.7 MHz, $CDCl_3$, 25 °C, PhTeTePh): δ = 432.3 ppm (s, $^1J(^{123}Te,^{125}Te)$ = 787 Hz).

An-pTeTeAn-p: ^{125}Te NMR (85.2 MHz, $CDCl_3$, 25 °C, PhTeTePh): δ = 461.3 ppm (s); ^{123}Te NMR (70.7 MHz, $CDCl_3$, 25 °C, PhTeTePh): δ = 461.0 ppm (s, $^1J(^{123}Te,^{125}Te)$ = 216 Hz).

An-oTeTeAn-o: ^{125}Te NMR (85.2 MHz, $CDCl_3$, 25 °C, PhTeTePh): δ = 175.9 ppm (s); ^{123}Te NMR (70.7 MHz, $CDCl_3$, 25 °C, PhTeTePh): δ = 175.9 ppm (s, $^1J(^{123}Te,^{125}Te)$ = 279 Hz).

TpTeTeTp: ^{125}Te NMR (85.2 MHz, $CDCl_3$, 25 °C, PhTeTePh): δ = 408.9 ppm (s); ^{123}Te NMR (70.7 MHz, $CDCl_3$, 25 °C, PhTeTePh): δ = 409.9 ppm (s, $^1J(^{123}Te,^{125}Te)$ = 198 Hz).

FpTeTeFp: ^{125}Te NMR (85.2 MHz, $CDCl_3$, 25 °C, PhTeTePh): δ = 463.1 ppm (s); ^{123}Te NMR (70.7 MHz, $CDCl_3$, 25 °C, PhTeTePh): δ = 463.9 ppm (s, $^1J(^{123}Te,^{125}Te)$ = 129 Hz).

MesTeTeMes: ^{125}Te NMR (85.2 MHz, $CDCl_3$, 25 °C, PhTeTePh): $\delta =$ 201.6(s); ^{123}Te NMR (70.7 MHz, $CDCl_3$, 25 °C, PhTeTePh): $\delta =$ 201.6 ppm (s, $^1J(^{123}Te,^{125}Te) = 532$ Hz).

TipTeTeTip: ^{125}Te NMR (85.2 MHz, $CDCl_3$, 25 °C, PhTeTePh): $\delta =$ 183.2 ppm (s); ^{123}Te NMR (70.7 MHz, $CDCl_3$, 25 °C, PhTeTePh): $\delta =$ 182.6 ppm (s, $^1J(^{123}Te,^{125}Te) = 650$ Hz).

1,8-Bis(4-fluorophenyltelluro)naphthalene [Nap(TeFp)$_2$] (N2)

A solution of *n*-butyllithium in hexane (2.5 M, 2.3 mL, 5.83 mmol) was added dropwise to a solution of 1,8-diiodonaphthalene (1.09 g, 2.87 mmol) in diethyl ether (50 mL) at −78 °C was added. The mixture was stirred at this temperature for 1 h after which a solution of bis(4-fluorophenyl) ditelluride (FpTeTeFp) (2.56 g, 5.74 mmol) in diethyl ether (200 mL) was added dropwise to the mixture. The resulting mixture was stirred at −78 °C for a further 2 h. The reaction mixture was washed with 0.1 M sodium hydroxide (2×200 mL). The organic layer was dried with magnesium sulfate, concentrated under reduced pressure, and purified by column chromatography on silica gel (hexane) to give the title compound as a brown solid. An analytically pure sample was obtained from recrystallisation by diffusion of hexane into a saturated solution of the compound in dichloromethane (1.07 g, 65 %). M.p. 98–100 °C; ^{1}H NMR (300 MHz, $CDCl_3$, 25 °C, Me_4Si): $\delta = 7.88$ (dd, $^3J(H,H) =$ 7.2 Hz, $^4J(H,H) = 1.2$ Hz, 2H; Nap 4,5-H), 7.54 (dd, $^3J(H,H) = 8.2$, $^4J(H,H) = 1.1$ Hz, 2H; Nap 2,7-H), 7.49–7.39 (m, 4H; Te*Fp* 10,14,16,20-H), 7.00 (dd, $^3J(H,H) = 8.0$,7.2 Hz, 2H; Nap 3,6-H), 6.75–6.65 ppm (m, 4H; Te*Fp* 11,13,17,19-H); ^{19}F NMR (282.3 MHz, $CDCl_3$, 25 °C, CCl_3F): $\delta = -113.1$ ppm (s); ^{125}Te NMR (85.2 MHz, $CDCl_3$, 25 °C, PhTeTePh): $\delta = 615.8$ ppm (s); ^{123}Te NMR (70.7 MHz, $CDCl_3$, 25 °C, PhTeTePh): $\delta = 616.1$ ppm (s, $^4J(^{123}Te,^{125}Te) = 2082$ Hz); MS (ES$^+$): *m/z* (%): 602.93 (100) [*M*+OMe$^+$]; elemental analysis calcd (%) for $C_{22}H_{14}F_2Te_2$: C 46.2, H 2.5; found: C 46.4, H 2.3.

1,8-Bis(4-methylphenyltelluro)naphthalene [Nap(TeTol)$_2$] (N3)

1,8-Bis(4-methylphenyltelluro)naphthalene [Nap(TeTol)$_2$] (**N3**) was prepared by following the procedure described previously for **N2** with 1,8-diiodonaphthalene (0.99 g, 2.63 mmol), a solution of *n*-butyllithium in hexane (2.5 M, 2.1 mL, 5.34 mmol) and (TolTeTeTol) (2.32 g, 5.26 mmol). The crude product was triturated with hexane to afford the target compound as a brown solid. An analytically pure sample was obtained from recrystallisation by diffusion of hexane into a saturated solution of the compound in dichloromethane (0.19 g, 13 %). M.p. 160–162 °C (decomp); ^{1}H NMR (300 MHz, $CDCl_3$, 25 °C, Me_4Si): $\delta = 8.08$ (dd, $^3J(H,H) = 7.2$, $^4J(H,H) = 1.2$ Hz, 2H; Nap 4,5-H), 7.74 (dd, $^3J(H,H) = 8.2$, $^4J(H,H) = 1.1$ Hz, 2H; Nap 2,7-H), 7.56 (d, $^3J(H,H) = 8.2$ Hz, 4H; Te*Tol* 11,13,18,20-H), 7.19 (dd, $^3J(H,H) =$ 8.0,7.2 Hz, 2H; Nap 3,6-H), 7.04 (d, $^3J(H,H) = 7.6$ Hz, 4H; Te*Tol* 10,14,17,21-H), 2.34 ppm (s, 6H; 2xTe*Tol* *p*-C*H*$_3$); ^{125}Te NMR (85.2 MHz, $CDCl_3$, 25 °C, PhTeTePh): $\delta = 607.6$ ppm (s); ^{123}Te NMR (70.7 MHz, $CDCl_3$, 25 °C, PhTeTePh): $\delta = 607.4$ ppm (s, $^4J(^{123}Te,^{125}Te) =$ 2145 Hz); MS (ES$^+$): *m/z* (%): 594.98 (100) [*M*+OMe$^+$]; elemental analysis calcd (%) for $C_{24}H_{20}Te_2$: C 51.1, H 3.6; found: C 50.9, H 3.5.

1,8-Bis(4-methoxyphenyltelluro)naphthalene [Nap(TeAn-*p*)$_2$] (N4)

1,8-Bis(4-methoxyphenyltelluro)naphthalene [Nap(TeAn-*p*)$_2$] (**N4**) was prepared following the procedure described previously for **N2**, with 1,8-diiodonaphthalene (0.95 g, 2.50 mmol), 2.5 M solution of *n*-butyllithium in hexane (2.0 mL, 5.10 mmol) and (An-*p*TeTeAn-*p*) (2.37 g, 5.00 mmol). The crude product was triturated with hexane to afford the purified target compound as a brown solid. An analytically pure sample was obtained from recrystallisation by diffusion of hexane into a saturated solution of the compound in dichloromethane (0.67 g, 45 %). M.p. 137–139 °C; ^{1}H NMR (300 MHz, $CDCl_3$, 25 °C, Me_4Si): $\delta = 7.94$ (dd, $^3J(H,H) = 7.2$, $^4J(H,H) = 1.2$ Hz, 2H; Nap 4,5-H), 7.60 (dd, $^3J(H,H) = 8.2$, $^4J(H,H) = 1.1$ Hz, 2H; Nap 2,7-H), 7.55 (d, $^3J(H,H) = 8.8$ Hz, 4H: Te*An-p* 11,13,18,20-H), 7.06 (dd, $^3J(H,H) = 8.0$,7.2 Hz, 2H; Nap 3,6-H), 6.67 (d, $^3J(H,H) = 8.8$ Hz, 4H; Te*An-p* 10,14,17,21-H), 3.69 ppm (s, 6H; 2×Te*An-p* OC*H*$_3$); ^{125}Te NMR (85.2 MHz, $CDCl_3$, 25 °C, PhTeTePh): $\delta = 601.9$ ppm (s); ^{123}Te NMR (70.7 MHz, $CDCl_3$, 25 °C, PhTeTePh): $\delta = 601.8$ ppm (s, $^4J(^{123}Te,^{125}Te) =$ 2189 Hz); MS (ES$^+$): *m/z* (%): 626.97 (40) [*M*+OMe$^+$], 612.96 (100) [*M*+OH$^+$]; elemental analysis calcd (%) for $C_{24}H_{20}O_2Te_2$: C 48.4, H 3.4; found: C 48.3, H 3.5.

1,8-Bis(2-methoxyphenyltelluro)naphthalene [Nap(TeAn-*o*)$_2$] (N5)

1,8-Bis(2-methoxyphenyltelluro)naphthalene [Nap(TeAn-*o*)$_2$] (**N5**) was prepared following the procedure described previously for **N2**, with 1,8-diiodonaphthalene (0.81 g, 2.12 mmol), a solution of *n*-butyllithium in hexane (2.5 M, 1.7 mL, 4.31 mmol) and (An-*o*TeTeAn-*o*) (2.01 g, 4.24 mmol). The crude product was purified by column chromatography on silica gel (hexane) to give the title compound as a brown solid. An analytically pure sample was obtained from recrystallisation by diffusion of hexane into a saturated solution of the compound in dichloromethane (0.19 g, 15 %). M.p. 58–60 °C; ^{1}H NMR (300 MHz, $CDCl_3$, 25 °C, Me_4Si): $\delta = 8.02$ (dd, $^3J(H,H) = 7.1$, $^4J(H,H) = 1.2$ Hz, 2H; Nap 4,5-H), 7.71 (dd, $^3J(H,H) = 8.2$, $^4J(H,H) =$ 1.1 Hz, 2H; Nap 2,7-H), 7.18–7.04 (m, 4H; Te*An-o* 13,19-H, Nap 3,6-H), 6.78–6.67 (m, 4H; Te*An-o* 11,14,17,20-H), 6.61–6.53 (m, 2H, Te*An-o* 12,18-H), 3.68 ppm (s, 6H; 2xTe*An-o* OC*H*$_3$); ^{125}Te NMR (85.2 MHz, $CDCl_3$, 25 °C, PhTeTePh): $\delta = 514.6$ ppm (s); ^{123}Te NMR (70.7 MHz, $CDCl_3$, 25 °C, PhTeTePh): $\delta = 514.0$ ppm (s, $^4J(^{123}Te,^{125}Te) =$ 2219 Hz); MS (ES$^+$): *m/z* (%): 626.99 (100) [*M*+OMe$^+$]; elemental analysis calcd (%) for $C_{24}H_{20}O_2Te_2$: C 48.4, H 3.4; found: C 48.5, H 3.3.

1,8-Bis(4-*tert*-butylphenyltelluro)naphthalene [Nap(TeTp)$_2$] (N6)

1,8-Bis(4-*tert*-butylphenyltelluro)naphthalene [Nap(TeTp)$_2$] (**N6**) was prepared by following the procedure described previously for **N2**, with 1,8-diiodonaphthalene (1.10 g, 2.90 mmol), a solution of *n*-butyllithium in hexane (2.5 M, 2.4 mL, 5.90 mmol) and (TpTeTeTp) (3.03 g, 5.81 mmol). The crude product was purified by column chromatography on silica gel (hexane) to give the title compound as a brown solid. An analytically pure sample was obtained from recrystallisation by diffusion of hexane into a saturated solution of the compound in $CDCl_3$ (0.96 g, 51 %). M.p. 72–74 °C; ^{1}H NMR (300 MHz, $CDCl_3$, 25 °C, Me_4Si): $\delta = 8.23$ (dd, $^3J(H,H) = 7.2$, $^4J(H,H) =$ 1.2 Hz, 2H; Nap 4,5-H), 7.79 (dd, $^3J(H,H) = 8.2$ Hz, $^4J(H,H) = 1.1$ Hz, 2H; Nap 2,7-H), 7.69 (d, $^3J(H,H) = 8.4$ Hz, 4H; Te*Tp*11,13,21,23-H), 7.33 (d, $^3J(H,H) = 8.4$ Hz, 4H; Te*Tp* 10,14,20,24-H), 7.24 (dd, $^3J(H,H) =$ 8.0,7.2 Hz, 2H; Nap 3,6-H), 1.41 ppm (s, 18H; 2×Te*Tp* *p*-*t*Bu); ^{125}Te NMR (85.2 MHz, $CDCl_3$, 25 °C, PhTeTePh): $\delta = 603.8$ ppm (s); ^{123}Te NMR (70.7 MHz, $CDCl_3$, 25 °C, PhTeTePh): $\delta = 604.9$ ppm (s, $^4J(^{123}Te,^{125}Te) = 2097$ Hz); MS (ES$^+$): *m/z* (%): 678.50 (100) [*M*+OMe$^+$]; elemental analysis calcd (%) for $C_{30}H_{32}Te_2$: C 55.6, H 5.0; found: C 55.7, H 4.9.

1,8-Bis(2,4,6-trimethylphenyltelluro)naphthalene [Nap(TeMes)$_2$] (N7)

1,8-Bis(2,4,6-trimethylphenyltelluro)naphthalene [Nap(TeMes)$_2$] (**N7**) was prepared following the procedure described previously for **N2**, with 1,8-diiodonaphthalene (0.92 g, 2.41 mmol), a solution of *n*-butyllithium in hexane (2.5 M, 2.0 mL, 4.89 mmol) and (MesTeTeMes) (2.40 g, 4.82 mmol). The crude product was purified by column chromatography on silica gel (hexane) to give a yellow solid. An analytically pure sample was obtained from recrystallisation by diffusion of hexane into a saturated solution of the compound in dichloromethane (0.17 g, 11%). M.p. 188–190 °C; ^{1}H NMR (300 MHz, $CDCl_3$, 25 °C, Me_4Si): $\delta = 7.57$ (dd, $^3J(H,H) = 7.2$, $^4J(H,H) = 1.2$ Hz, 2H; Nap 4,5-H), 7.51 (dd, $^3J(H,H) = 8.2$, $^4J(H,H) = 1.1$ Hz, 2H; Nap 2,7-H), 6.92 (m, 2H; Nap 3,6-H), 6.82 (s, 4H; Te*Mes* 11,13,20,22-H), 2.27 (s, 12H, 4×Te*Mes* *o*-CH_3), 2.18 ppm (s, 6H; 2×Te*Mes* *p*-CH_3); ^{125}Te NMR (85.2 MHz, $CDCl_3$, 25 °C, PhTeTePh): $\delta = 397.4$ ppm (s); ^{123}Te NMR (70.7 MHz, $CDCl_3$, 25 °C, PhTeTePh): $\delta = 396.7$ ppm (s, $^4J(^{123}Te,^{125}Te) = 3191$ Hz); MS (ES$^+$): *m/z* (%): 651.05 (100) [*M*+OMe$^+$]; elemental analysis calcd (%) for $C_{28}H_{28}Te_2$: C 54.3, H 4.6; found: C 54.3, H 4.7.

1,8-Bis(2,4,6-triisopropanylphenyltelluro)naphthalene [Nap(TeTip)$_2$] (N8)

1,8-Bis(2,4,6-triisopropanylphenyltelluro)naphthalene [Nap(TeTip)$_2$] (**N8**) was prepared following the procedure described previously for **N2**, with 1,8-diiodonaphthalene (0.98 g, 2.58 mmol), a solution of *n*-butyllithium in hexane (2.5 M, 2.1 mL, 5.24 mmol) and (TipTeTeTip) (3.41 g, 5.16 mmol). The crude product was purified by column chromatography on silica gel (hexane) to give the title compound as a yellow oil (0.53 g, 26%). M.p. 48–50 °C; ^{1}H NMR (300 MHz, $CDCl_3$, 25 °C, Me_4Si): $\delta = 7.91$ (dd, $^3J(H,H) = 7.2$, $^4J(H,H) = 1.0$ Hz, 2H; Nap 4,5-H), 7.75 (dd, $^3J(H,H) = 8.1$, $^4J(H,H) = 1.0$ Hz, 2H; Nap 2,7-H), 7.28 (s, 4H; Te*Tip* 11,13,26,28,-H), 7.22–7.14 (m, 2H; Nap 3,6-H), 3.98 (septet, $^3J(H,H) = 6.8$ Hz, 4H; Te*Tip* *o*-$CHMe_2$), 3.13 (septet, $^3J(H,H) = 6.9$ Hz, 2H; Te*Tip* *p*-$CHMe_2$), 1.49 (d, $^3J(H,H) = 6.9$ Hz, 12H; Te*Tip* *p*-$CHMe_2$), 1.29 ppm (d, $^3J(H,H) = 6.8$ Hz, 24H; Te*Tip* *o*-$CHMe_2$); ^{125}Te NMR (85.2 MHz, $CDCl_3$, 25 °C, PhTeTePh): $\delta = 346.4$ ppm (s); ^{123}Te NMR (70.7 MHz, $CDCl_3$, 25 °C, PhTeTePh): $\delta = 346.1$ ppm (s, $^4J(^{123}Te,^{125}Te) = 3095$ Hz); MS (ES$^+$): *m/z* (%): 819.23 (100) [*M*+OMe$^+$], 805.22 (60) [*M*+OH$^+$]; elemental analysis calcd (%) for $C_{40}H_{52}Te_2$: C 61.0, H 6.65; found: C 60.8, H 6.7.

5,6-Bis(4-fluorophenyltelluro)acenaphthene [Acenap(TeFp)$_2$] (A2)

A solution of 5,6-dibromoacenaphthene (1.17 g, 3.74 mmol) in diethyl ether (40 mL) was cooled to −10–0 °C on an ice-ethanol bath and to this was added a solution of tetramethylethylenediamine (TMEDA) (1.7 mL, 9.92 mmol). The mixture was allowed to stir for 15 min before a solution of *n*-butyllithium (2.5 M) in hexane (3.6 mL, 8.97 mmol) was added dropwise over a period of 15 min. During these operations, the temperature of the mixture was maintained at −10–0 °C. The mixture was stirred at this temperature for a further 1 h, before being cooled to −78 °C. A solution of bis(4-fluorophenyl) ditelluride (FpTeTeFp) (3.33 g, 7.47 mmol) in diethyl ether (150 mL) was then added dropwise and the resulting solution was stirred at −78 °C for a further 2 h. The mixture was allowed to warm to room temperature and then washed with 0.1 N sodium hydroxide (2×60 mL). The organic layer was dried over magnesium sulfate and concentrated under reduced pressure to afford a red solid. The crude product was washed with hexane affording a cream solid which was collected by filtration. An analytically pure sample was obtained from recrystallisation by diffusion of hexane into a saturated solution of the compound in dichloromethane (1.21 g, 54%). M.p. 140–142 °C; ^{1}H NMR (300 MHz, $CDCl_3$, 25 °C, Me_4Si): $\delta = 7.73$ (d, $^3J(H,H) = 7.2$ Hz, 2H; Acenap 4,7-H), 7.60–7.50 (m, 4H; Te*Fb* 12,16,18,22-H), 6.94 (d, $^3J(H,H) = 7.2$ Hz, 2H; Acenap 3,8-H), 6.85–6.74 (m, 4H; Te*Fb* 13,15,19,21-H), 3.22 ppm (s, 4H, 2×CH_2); ^{19}F NMR (282.3 MHz, $CDCl_3$, 25 °C, CCl_3F): $\delta = -113.6$ ppm (s); ^{125}Te NMR (85.2 MHz, $CDCl_3$, 25 °C, PhTeTePh): $\delta = 581.7$ ppm (s); ^{123}Te NMR (70.7 MHz, $CDCl_3$, 25 °C, PhTeTePh): $\delta = 579.9$ ppm (s, $^4J(^{123}Te,^{125}Te) = 1746$ Hz); MS (ES$^+$): *m/z* (%): 628.95 (100) [*M*+OMe$^+$]; elemental analysis calcd (%) for $C_{24}H_{16}F_2Te_2$: C 48.2, H 2.7; found: C 48.3, H 2.6.

5,6-Bis(4-methylphenyltelluro)acenaphthene [Acenap(TeTol)$_2$] (A3)

5,6-Bis(4-methylphenyltelluro)acenaphthene [Acenap(TeTol)$_2$] (**A3**) was prepared following the procedure described previously for **A2**, with 5,6-dibromoacenaphthene (0.36 g, 1.14 mmol), TMEDA (0.5 mL, 3.03 mmol), a solution of *n*-butyllithium (2.5 M) in hexane (1.1 mL, 2.74 mmol) and (TolTeTeTol) (1.01 g, 2.28 mmol). The crude product was washed with hexane affording a yellow solid which was collected by filtration. An analytically pure sample was obtained from recrystallisation by diffusion of hexane into a saturated solution of the compound in dichloromethane (0.26 g, 38%). M.p. 155–157 °C; ^{1}H NMR (300 MHz, $CDCl_3$, 25 °C, Me_4Si): $\delta = 7.78$ (d, $^3J(H,H) = 7.2$ Hz, 2H; Acenap 4,7-H), 7.55–7.46 (m, 4H; Te*Tol* 12,16,18,22-H), 6.98–6.89 (m, 6H; Acenap 3,8-H, Te*Tol* 13,15,19,21-H), 3.23 (s, 4H; 2×CH_2), 2.23 ppm (s, 6H; 2×CH_3); ^{125}Te NMR (85.2 MHz, $CDCl_3$, 25 °C, PhTeTePh): $\delta = 574.4$ ppm (s); ^{123}Te NMR (70.7 MHz, $CDCl_3$, 25 °C, PhTeTePh): $\delta = 574.1$ ppm (s, $^4J(^{123}Te,^{125}Te) = 1781$ Hz); MS (ES$^+$): *m/z* (%): 606.98 (100) [*M*+OH$^+$]; elemental analysis calcd (%) for $C_{26}H_{22}Te_2$: C 53.0, H 3.8; found: C 52.7, H 3.8.

5,6-Bis(4-methoxyphenyltelluro)acenaphthene [Acenap(TeAn-p)$_2$] (A4)

5,6-Bis(4-methoxyphenyltelluro)acenaphthene [Acenap(TeAn-p)$_2$] (**A4**) was prepared following the procedure described previously for **A2**, with 5,6-dibromoacenaphthene (0.36 g, 1.16 mmol), TMEDA (0.5 mL, 3.09 mmol), a solution of *n*-butyllithium (2.5 M) in hexane (1.1 mL, 2.79 mmol) and (An-*p*TeTeAn-*p*) (1.10 g, 2.33 mmol). The crude product was washed with hexane affording a brown solid which was collected by filtration. An analytically pure sample was obtained from recrystallisation by diffusion of hexane into a saturated solution of the compound in dichloromethane (0.39 g, 53%). M.p. 140–142 °C (decomp); ^{1}H NMR (300 MHz, $CDCl_3$, 25 °C, Me_4Si): $\delta = 7.88$ (d, $^3J(H,H) = 7.3$ Hz, 2H; Acenap 4,7-H), 7.75–7.66 (m, 4H; TeAn-*p* 12,16,18,22-H), 7.06 (d, $^3J(H,H) = 7.3$ Hz, 2H; Acenap 3,8-H), 6.84–6.77 (m, 4H; TeAn-*p* 13,15,19,21-H), 3.82 (s, 6H, 2×TeAn-*p* OCH_3), 3.35 ppm (s, 4H, 2×CH_2); ^{125}Te NMR (85.2 MHz, $CDCl_3$, 25 °C, PhTeTePh): $\delta = 567.8$ ppm (s); ^{123}Te NMR (70.7 MHz, $CDCl_3$, 25 °C, PhTeTePh): $\delta = 567.8$ ppm (s, $^4J(^{123}Te,^{125}Te) = 1835$ Hz); MS (ES$^+$): *m/z* (%): 652.99 (72) [*M*+OMe$^+$], 638.97 (100) [*M*+OH$^+$]; elemental analysis calcd (%) for $C_{26}H_{22}O_2Te_2$: C 50.2, H 3.6; found: C 50.0, H 3.6.

5,6-Bis(2-methoxyphenyltelluro)acenaphthene [Acenap(TeAn-o)$_2$] (A5)

5,6-Bis(2-methoxyphenyltelluro)acenaphthene [Acenap(TeAn-o)$_2$] (**A5**) was prepared following the procedure described previously for **A2**, with 5,6-dibromoacenaphthene (1.32 g, 4.24 mmol), TMEDA (1.8 mL, 11.27 mmol), a solution of *n*-butyllithium (2.5 M) in hexane (4.1 mL, 10.19 mmol) and (An-*o*TeTeAn-*o*) (4.02 g, 8.48 mmol). The

crude product was washed with hexane affording a cream solid which was collected by filtration. An analytically pure sample was obtained from recrystallisation by diffusion of hexane into a saturated solution of the compound in dichloromethane (1.03 g, 39%). M.p. 75–77 °C; ^{1}H NMR (300 MHz, $CDCl_3$, 25 °C, Me_4Si): $\delta = 7.94$ (d, $^3J(H,H) = 7.2$ Hz, 2H; Acenap 4,7-H), 7.31–7.20 (m, 2H; TeAn-*o* 15,22-H), 7.16–7.06 (m, 4H; TeAn-*o* 13,20-H, Acenap 3,8-H), 6.87 (dd, $^3J(H,H) = 8.2$, $^4J(H,H) = 0.8$ Hz, 2H; TeAn-*o* 16,23-H), 6.79–6.69 (m, 2H; TeAn-*o* 14,21-H), 3.86 (s, 6H; 2×TeAn-*o* OCH_3), 3.42 ppm (s, 4H; 2×CH_2); ^{125}Te NMR (85.2 MHz, $CDCl_3$, 25 °C, PhTeTePh): $\delta =$ 482.4 ppm (s); ^{123}Te NMR (70.7 MHz, $CDCl_3$, 25 °C, PhTeTePh): $\delta =$ 481.9 ppm (s, $^4J(^{123}Te,^{125}Te) = 1796$ Hz); MS (ES^+): *m/z* (%): 652.98 (100) [*M*+OMe^+]; elemental analysis calcd (%) for $C_{26}H_{22}O_2Te_2$: C 50.2, H 3.6; found: C 50.0, H 3.6.

5,6-Bis(4-*tert*-butylphenyltelluro)acenaphthene [Acenap(TeTp)$_2$] (A6)

5,6-Bis(4-*tert*-butylphenyltelluro)acenaphthene [Acenap(TeTp)$_2$] (**A6**) was prepared following the procedure described previously for **A2** with 5,6-dibromoacenaphthene (1.10 g, 3.53 mmol), TMEDA (1.6 mL, 9.37 mmol), a solution of *n*-butyllithium (2.5 M) in hexane (3.4 mL, 8.48 mmol) and (TpTeTeTp) (3.68 g, 7.06 mmol). The crude product was purified by column chromatography on silica gel (hexane) to give the title compound as a brown solid. An analytically pure sample was recrystallised by diffusion of hexane into a saturated solution of the compound in dichloromethane (1.56 g, 61%). M.p. 55–57 °C; ^{1}H NMR (300 MHz, $CDCl_3$, 25 °C, Me_4Si): $\delta =$ 7.83 (d, $^3J(H,H) = 7.3$ Hz, 2H; Acenap 4,7-H), 7.54 (d, $^3J(H,H) = 8.4$ Hz, 4H; Te*Tp* 13,15,23,25-H), 7.34 (d, $^3J(H,H) = 8.4$ Hz, 4H; Te*Tp* 12,16,22,26-H), 6.96 (d, $^3J(H,H) = 7.3$ Hz, 2H; Acenap 3,8-H), 3.24 (s, 4H; 2×CH_2), 1.21 ppm (s, 18H; 2×*p*-*t*Bu); ^{125}Te NMR (85.2 MHz, $CDCl_3$, 25 °C, PhTeTePh): $\delta = 571.4$ ppm (s); ^{123}Te NMR (70.7 MHz, $CDCl_3$, 25 °C, PhTeTePh): $\delta = 571.6$ ppm (s, $^4J(^{123}Te,^{125}Te) = 1766$ Hz); MS (ES^+): *m/z* (%): 705.09 (100) [*M*+OMe^+]; elemental analysis calcd (%) for $C_{32}H_{34}Te_2$: C 57.0, H 5.1; found: C 56.8, H 5.0.

5,6-Bis(2,4,6-trimethylphenyltelluro)acenaphthene [Acenap(TeMes)$_2$] (A7)

5,6-Bis(2,4,6-trimethylphenyltelluro)acenaphthene [Acenap(TeMes)$_2$] (**A7**) was prepared following the procedure described previously for **A2**, with 5,6-dibromoacenaphthene (0.23 g, 0.96 mmol), TMEDA (0.4 mL, 2.55 mmol), a solution of *n*-butyllithium in hexane (2.5 M, 0.9 mL, 2.31 mmol) and (MesTeTeMes) (0.96 g, 1.92 mmol). The crude product was washed with hexane affording a yellow crystalline solid that was collected by filtration. An analytically pure sample was obtained from recrystallisation by diffusion of hexane into a saturated solution of the compound in dichloromethane (0.14 g, 22%). M.p. 125–127 °C (decomp). ^{1}H NMR (300 MHz, $CDCl_3$, 25 °C, Me_4Si): $\delta = 7.33$ (d, $^3J(H,H) = 7.3$ Hz, 2H; Acenap 4,7-H), 6.80 (s, 4H; Te*Mes* 13,15,18,22-H), 6.75 (d, $^3J(H,H) = 7.3$ Hz, 2H; Acenap 3,8-H), 3.12 (s, 4H, 2×CH_2), 2.30 (s, 12H; 4×CH_3), 2.15 ppm (s, 6H; 2×CH_3); ^{125}Te NMR (85.2 MHz, $CDCl_3$, 25 °C, PhTeTePh): $\delta =$ 363.3 ppm (s); ^{123}Te NMR (70.7 MHz, $CDCl_3$, 25 °C, PhTeTePh): $\delta =$ 362.9 ppm (s, $^4J(^{123}Te,^{125}Te) = 2819$ Hz); MS (ES^+): *m/z* (%): 677.06 (100) [*M*+OMe^+]; elemental analysis calcd (%) for $C_{30}H_{30}Te_2$: C 55.8, H 4.7; found: C 55.6, H 4.6.

5,6-Bis(2,4,6-triisopropanylphenyltelluro)acenaphthene [Acenap(TeTip)$_2$] (A8)

5,6-Bis(2,4,6-triisopropanylphenyltelluro)acenaphthene [Acenap(TeTip)$_2$] (**A8**) was prepared following the procedure described previously for **A2**, with 5,6-dibromoacenaphthene (1.13 g, 3.63 mmol), TMEDA (1.5 mL, 9.55 mmol), a solution of *n*-butyllithium (2.5 M) in hexane (3.5 mL, 8.63 mmol) and (TipTeTeTip) (4.78 g, 7.23 mmol). The crude product was purified by column chromatography on silica gel (hexane) to give the title compound as a brown solid. An analytically pure sample was recrystallised from hexane (1.60 g, 54%). M.p. 164–166 °C (decomp); ^{1}H NMR (300 MHz, $CDCl_3$, 25 °C, Me_4Si): $\delta = 7.69$ (d, $^3J(H,H) = 7.3$ Hz, 2H; Acenap 4,7-H), 7.27 (s, 4H; Te*Tip* 13,15,28,30-H), 7.07 (d, $^3J(H,H) = 7.3$ Hz, 2H; Acenap 3,8-H), 4.02 (septet, $^3J(H,H) = 6.8$ Hz, 4H; Te*Tip* *o*-$CHMe_2$), 3.39 (s, 4H; Acenap 2×CH_2), 3.12 (septet, $^3J(H,H) = 6.9$ Hz, 2H; Te*Tip* *p*-$CHMe_2$), 1.49 (d, $^3J(H,H) = 6.9$ Hz, 12H; Te*Tip* *p*-$CHMe_2$), 1.31 ppm (d, $^3J(H,H) = 6.8$ Hz, 24H; Te*Tip* *o*-$CHMe_2$); ^{125}Te NMR (85.2 MHz, $CDCl_3$, 25 °C, PhTeTePh): $\delta = 316.0$ ppm (s); ^{123}Te NMR (70.7 MHz, $CDCl_3$, 25 °C, PhTeTePh): $\delta = 315.8$ ppm (s, $^4J(^{123}Te,^{125}Te) = 2727$ Hz); MS (ES^+): *m/z* (%): 847.23 (100) [*M*+H_2OMe^+], 831.23 (85) [*M*+OH^+], 814.23 (20) [M^+]; elemental analysis calcd (%) for $C_{42}H_{52}Te_2$: C 62.0, H 6.7; found: C 62.0, H 6.4.

5,6-Bis(4-fluorophenyltelluro)acenaphthylene [Acenapyl(TeFp)$_2$] (Ay2)

2,3-Dichloro-5,6-dicyano-1,4-benzoquinone (DDQ) (1.5 g, 6.65 mmol) was added in one batch to a stirred solution of 5,6-bis(4-fluorophenyltelluro)acenaphthene (**A2**) (2.65 g, 4.43 mmol) in benzene (200 mL) and the mixture heated under reflux for 24 h. After cooling to room temperature, pentane (200 mL) was added and the mixture was filtered. The filtrate was passed through a short column of silica with a pentane eluent and concentrated under reduced pressure to yield the title compound as an orange solid. An analytically pure sample was obtained from recrystallisation by diffusion of hexane into a saturated solution of the compound in dichloromethane (0.48 g, 18%). M.p. 150–152 °C; ^{1}H NMR (300 MHz, $CDCl_3$, 25 °C, Me_4Si): $\delta = 7.71$ (d, $^3J(H,H) = 7.2$ Hz, 2H; Acenapyl 4,7-H), 7.62–7.57 (m, 4H; Te*Fp* 12,16-H), 7.17 (d, $^3J(H,H) =$ 7.2 Hz, 2H; Acenapyl 3,8-H), 6.86–6.79 (m, 6H; Te*Fp* 13–15-H), 6.75 ppm (s, 2H, Acenapyl 2×CH); ^{19}F NMR (282.3 MHz, $CDCl_3$, 25 °C, CCl_3F): $\delta = -112.9$ ppm (s); ^{125}Te NMR (85.2 MHz, $CDCl_3$, 25 °C, PhTeTePh): $\delta = 610.3$ ppm (s); ^{123}Te NMR (70.7 MHz, $CDCl_3$, 25 °C, PhTeTePh): $\delta = 610.1$ ppm (s, $^4J(^{123}Te,^{125}Te) = 1700$ Hz); MS (ES^+): *m/z* (%): 628.93 (100) [*M*+OMe^+], 614.92 (93) [*M*+OH^+]; elemental analysis calcd (%) for $C_{24}H_{14}F_2Te_2$: C 48.4, H 2.4; found C 48.2, H 2.3.

5,6-Bis(4-methylphenyltelluro)acenaphthylene [Acenapyl(TeTol)$_2$] (Ay3)

5,6-Bis(4-methylphenyltelluro)acenaphthylene [Acenapyl(TeTol)$_2$] (**Ay3**) was prepared following the procedure described previously for **Ay2**, with DDQ (0.32 g, 1.41 mmol) and [Acenap(TeTol)$_2$] **A3** (0.56 g, 0.94 mmol), yielding a red solid, which was recrystallized by evaporation of a dichloromethane solution of the product to afford red crystals (0.13 g, 23%). M.p. 180–182 °C; ^{1}H NMR (300 MHz, $CDCl_3$, 25 °C, Me_4Si): $\delta = 7.79$ (d, $^3J(H,H) = 7.2$ Hz, 2H; Acenapyl 4,7-H), 7.59 (d, $^3J(H,H) = 8.0$, 2H; Te*Tol* 12,16-H), 7.22 (d, $^3J(H,H) = 7.2$, 2H; Acenapyl 3,8-H), 7.00 (d, $^3J(H,H) = 7.6$, 2H; Te*Tol* 13,15-H), 6.78 (s, 2H; Acenapyl 2×CH), 2.28 ppm (s, 6H; Te*Tol* 2×CH_3); ^{125}Te NMR (85.2 MHz, $CDCl_3$, 25 °C, PhTeTePh): $\delta = 605.7$ ppm (s); ^{123}Te NMR (70.7 MHz, $CDCl_3$, 25 °C, PhTeTePh): $\delta = 605.9$ ppm (s, $^4J(^{123}Te,^{125}Te) = 1785$ Hz); MS (ES^+): *m/z* (%): 618.98 (100) [*M*+OMe^+]; elemental analysis calcd (%) for $C_{26}H_{20}Te_2$: C 53.1; H 3.4; found C 52.9, H 3.4.

5,6-Bis(4-methylphenyltelluro)acenaphthylene [Acenapyl(TeAn-*p*)$_2$] (Ay4)

5,6-Bis(4-methylphenyltelluro)acenaphthylene [Acenapyl(TeAn-*p*)$_2$] (**Ay4**) was prepared following the procedure described previously for **Ay2**, with DDQ (0.32 g, 1.41 mmol) and [Acenap(TeAn-*p*)$_2$] **A4** (0.56 g, 0.94 mmol), yielding a red solid, which was recrystallized by evaporation of a dichloromethane solution of the product to afford red crystals (0.13 g, 23%). M.p. 180–182 °C; ^{1}H NMR (300 MHz, $CDCl_3$, 25 °C, Me_4Si): $\delta = 7.79$ (d, ^3J(H,H) = 7.2 Hz, 2H; Acenapyl 4,7-H), 7.59 (d, ^3J(H,H) = 8.0, 2H; Te*An-p* 12,16-H), 7.22 (d, ^3J(H,H) = 7.2, 2H; Acenapyl 3,8-H), 7.00 (d, ^3J(H,H) = 7.6, 2H; Te*An-p* 13,15-H), 6.78 (s, 2H; Acenapyl 2x*CH*), 2.28 ppm (s, 6H; Te*An-p* 2× CH_3); ^{125}Te NMR (85.2 MHz, $CDCl_3$, 25 °C, PhTeTePh): $\delta = 605.7$ ppm (s); ^{123}Te NMR (70.7 MHz, $CDCl_3$, 25 °C, PhTeTePh): $\delta = 605.9$ ppm (s, ^4J(^{123}Te,^{125}Te) = 1785 Hz); MS (ES^+): *m/z* (%): 618.98 (100) [*M*+OMe^+]; elemental analysis calcd (%) for $C_{26}H_{20}Te_2$: C 53.1; H 3.4; found C 52.9, H 3.4.

5,6-Bis(4-*tert*-butylphenyltelluro)acenaphthylene [Acenapyl(TeTp)$_2$] (Ay6)

5,6-Bis(4-*tert*-butylphenyltelluro)acenaphthylene [Acenapyl(TeTp)$_2$] (**Ay6**) was prepared following the procedure described previously for **Ay2**, with DDQ (1.06 g, 4.66 mmol) and [Acenap(TeTp$_2$] **A6** (2.00 g, 2.97 mmol), yielding a red solid, which was recrystallized by evaporation of a chloroform solution of the product to afford red crystals (0.23 g, 12%). M.p. 187–189 °C; ^{1}H NMR (300 MHz, $CDCl_3$, 25 °C, Me_4Si): $\delta = 7.83$ (d, ^3J(H,H) = 7.2 Hz, 2H; Acenapyl 4,7-H), 7.61 (d, ^3J(H,H) = 8.3 Hz, 2H; Te*Tp* 12,16-H), 7.24–7.18 (m, 4H; Acenapyl 3,8-H, Te*Tp* 13,15-H), 6.77 (s, 2H; Acenapyl 2×*CH*), 1.22 ppm (s, 18H; Te*Tp* 2×*p*-*t*Bu); ^{125}Te NMR (85.2 MHz, $CDCl_3$, 25 °C, PhTeTePh): $\delta = 600.5$ ppm (s); ^{123}Te NMR (70.7 MHz, $CDCl_3$, 25 °C, PhTeTePh): $\delta = 600.7$ ppm (s, ^4J(^{123}Te,^{125}Te) = 1772 Hz); MS (ES^+): *m/z* (%): 703.08 (100) [*M*+OMe^+]; elemental analysis calcd (%) for $C_{32}H_{32}Te_2$: C 57.2; H 4.8; found C 57.1, H 4.9.

5,6-Bis(2,4,6-trimethylphenyltelluro)acenaphthylene [Acenapyl(TeMes)$_2$] (Ay7)

5,6-Bis(2,4,6-trimethylphenyltelluro)acenaphthylene [Acenapyl(-TeMes)$_2$] (**Ay7**) was prepared following the procedure described previously for **Ay2**, with DDQ (0.19 g, 0.83 mmol) and [Acenap(-TeMes)$_2$] **A7** (0.36 g, 0.55 mmol), to yield a red solid that was recrystallized by evaporation of a dichloromethane solution of the product affording red crystals (0.03 g, 9%). M.p. 171–173 °C (decomp); ^{1}H NMR (300 MHz, $CDCl_3$, 25 °C, Me_4Si): $\delta = 7.31$ (d, ^3J(H,H) = 7.3, 2H; Acenapyl 4,7-H), 7.06 (d, ^3J(H,H) = 7.2, 2H; Acenapyl 3,8-H), 6.90 (s, 2H; Te*Mes* 13,15-H), 6.70 (s, 2H; 2×*CH*), 2.42 (s, 6H; Te*Mes* 2×CH_3), 2.22 ppm (s, 3H; Te*Mes* 1×CH_3); ^{125}Te NMR (85.2 MHz, $CDCl_3$, 25 °C, PhTeTePh): $\delta = 406.9$ ppm (s); ^{123}Te NMR (70.7 MHz, $CDCl_3$, 25 °C, PhTeTePh): $\delta = 406.3$ ppm (s, ^4J(^{123}Te,^{125}Te) = 2956 Hz); MS (ES^+): *m/z* (%): 690.94 (100) [*M*+Na_2^+], 674.96 (55) [*M*+OMe^+]; elemental analysis calcd (%) for $C_{30}H_{28}Te_2$: C 56.0, H 4.4; found C 55.9, H 4.5.

5,6-Bis(2,4,6-triisopropanylphenyltelluro)acenaphthylene [Acenapyl(TeTip)$_2$] (Ay8)

5,6-Bis(2,4,6-triisopropanylphenyltelluro)acenaphthylene [Acenapyl(TeTip)$_2$] (**Ay8**) was prepared following the procedure described previously for **Ay2**, with DDQ (0.66 g, 2.91 mmol) and [Acenap(TeTip)$_2$] **A8** (1.56 g, 1.92 mmol), to yield an orange solid that was recrystallized by evaporation of a dichloromethane solution of the product affording orange crystals (0.21 g, 14%). M.p. 75–77 °C; ^{1}H NMR (300 MHz, $CDCl_3$, 25 °C, Me_4Si): $\delta = 7.58$ (d, ^3J(H,H) = 7.3 Hz, 2H; Acenapyl 4,7-H), 7.32 (d, ^3J(H,H) = 7.3 Hz, 2H; Acenapyl 3,8-H), 7.27 (s, 4H; Te*Tip* 13,15,28,30-H), 6.92 (s, 2H; Acenapyl 9,10-H), 3.09 (septet, ^3J(H,H) = 6.7 Hz, 4H; Te*Tip* *o*-*CH*Me_2), 3.92 (septet, ^3J(H,H) = 6.9 Hz, 4H; Te*Tip* *p*-*CH*Me_2), 1.45 (d, ^3J(H,H) = 6.9 Hz, 12H; Te*Tip* *p*-*CH*Me_2), 1.30 ppm (d, ^3J(H,H) = 6.8 Hz, 24H; Te*Tip* *o*-*CH*Me_2); ^{125}Te NMR (85.2 MHz, $CDCl_3$, 25 °C, PhTeTePh): $\delta = 353.7$ ppm (s); ^{123}Te NMR (70.7 MHz, $CDCl_3$, 25 °C, PhTeTePh): $\delta = 353.3$ ppm (s, ^4J(^{123}Te,^{125}Te) = 2958 Hz); MS (ES^+): *m/z* (%): 833.19 (100) [*M*+Na^+]; elemental analysis calcd (%) for $C_{42}H_{52}Te_2$: C 62.1, H 6.45; found C 62.25, H 6.4.

Crystal structure analyses

X-ray crystal structures for **N3**, **N4**, **N5**, **N7**, **A8**, **Ay2** and **Ay8** were determined at −148(1) °C using a Rigaku MM007 high-brilliance RA generator (Mo Kα radiation, confocal optic) and Saturn CCD system. At least a full hemisphere of data was collected using ω scans. Intensities were corrected for Lorentz, polarization, and absorption. Data for compounds **N2**, **N6**, **A2**, **A6** and **Ay6** were collected at −100(1) °C and for **A5**, **Ay3**, **Ay4** and **Ay7** at −180(1) °C using a Rigaku MM007 high-brilliance RA generator ($Mo_{K\alpha}$ radiation, confocal optic) and Mercury CCD system. At least a full hemisphere of data was collected using ω scans. Data for **A3** and **A4** were determined at −148(1) °C with the St Andrews Robotic Diffractometer,[25] a Rigaku ACTOR-SM, and a Saturn 724 CCD area detector with graphite-monochromated $Mo_{K\alpha}$ radiation (λ = 0.71073 Å). Data were corrected for Lorentz, polarisation and absorption. Data for all compounds analyzed were collected and processed using CrystalClear (Rigaku).[26] Structures were solved by direct methods[27] and expanded using Fourier techniques.[28] Non-hydrogen atoms were refined anisotropically. Hydrogen atoms were refined using the riding model. All calculations were performed using the CrystalStructure[29] crystallographic software package except for refinement, which was performed using SHELXL2013.[30]

CCDC-1027368 (**A2**), -1027388 (**A3**), -1027390 (**A4**), 1027391 (**A5**), 1027393 (**A6**), -1027369 (**A8**), -1027371 (**Ay2**), -1027373 (**Ay3**), -1027375 (**Ay4**), -1027377 (**Ay6**), -1027379 (**Ay7**), -1027381 (**Ay8**), -1027383 (**N2**), -1027385 (**N3**), -1027396 (**N4**), 1027398 (**N5**), -1027400 (**N6**), 1027402 (**N7**). contain the supplementary crystallographic data for this paper. These data can be obtained free of charge from The Cambridge Crystallographic Data Centre via www.ccdc.cam.ac.uk/data_request/cif.

Solid-state NMR spectroscopy

^{125}Te solid-state NMR spectroscopic experiments were performed using a Bruker Avance III spectrometer operating at a magnetic field strengths of either 9.4 or 14.1 T, corresponding to a ^{125}Te Larmor frequency of 126.2 MHz. Experiments were carried out using conventional 4- and 1.9 mm MAS probes, with MAS rates between 14 and 40 kHz. Chemical shifts are referenced relative to $(CH_3)_2Te$ at 0 ppm, using the isotropic resonance of solid $Te(OH)_6$ (site 1) at 692.2 ppm as a secondary reference. Transverse magnetization was obtained by cross polarization (CP) from ^{1}H using optimized contact pulse durations of 8 ms, and two-pulse phase modulation (TPPM) ^{1}H decoupling during acquisition. Spectra were acquired with a recycle interval of 50 and 55 s. The position of the isotropic resonances within the spinning sidebands patterns were unambiguously determined by recording a second spectrum at a higher MAS rate. A more detailed description of the experimental

parameters for individual materials is given in the Supporting Information.

Computational details

The same levels were employed as in our recent study on perinaphthyl ditellurides,[11] that is, geometry optimisations were carried out at the B3LYP/6-31G* level (SDD pseudopotential with augmented valence basis on Te), *J* values computed[30] at the ZORA-Spinorbit/BP86/TZ2P level (which has performed well for the computation of SSCCs involving fourth-row and heavier elements).[31] See the Supporting Information for further details and references.

Acknowledgements

Elemental analyses were performed by Stephen Boyer at the London Metropolitan University. Mass spectrometry was performed by Caroline Horsburgh at the University of St. Andrews Mass Spectrometry Service. The author(s) would like to acknowledge the use of the EPSRC UK National Service for Computational Chemistry Software (NSCCS) at Imperial College London in carrying out this work. Calculations were performed using the EaStCHEM Research Computing Facility maintained by Dr. H. Früchtl and a Silicon Graphics Altix cluster at NSCCS. The work in this project was supported by the Engineering and Physical Sciences Research Council (EPSRC). M.B. wishes to thank EaStCHEM and the University of St Andrews for support.

Keywords: bis(tellurides) · conformational dependence · DFT calculations · NMR spectroscopy · spin–spin coupling · X-ray crystallography

[1] J.-C. Hierso, *Chem. Rev.* **2014**, *114*, 4838.
[2] W. Kemp, *NMR in Chemistry, A Multinuclear Introduction*, Macmillan Education Ltd, Hampshire, England, **1986**.
[3] R. V. Parish in *NMR, NQR, EPR, and Mössbauer Spectroscopy in Inorganic Chemistry* (Ed. J. Burgess), Ellis Horwood, Chichester, England, **1990**.
[4] L. Ernst, P. Sakhaii, *Magn. Reson. Chem.* **2000**, *38*, 559.
[5] L. Ernst, K. Ibrom, *Angew. Chem.* **1995**, *107*, 2010; *Angew. Chem. Int. Ed. Engl.* **1995**, *34*, 1881.
[6] F. B. Mallory, C. W. Mallory, K. E. Butler, M. Beth Lewis, A. Qian Xia, E. D. Luzik, Jr., L. E. Fredenburgh, M. M. Ramanjulu, Q. N. Van, M. M. Francl, D. A. Freed, C. C. Wray, C. Hann, M. Nerz-Stormes, P. J. Carroll, L. E. Chirlian, *J. Am. Chem. Soc.* **2000**, *122*, 4108.
[7] J. E. Peralta, V. Barone, R. H. Contreras, D. G. Zaccari, J. P. Snyder, *J. Am. Chem. Soc.* **2001**, *123*, 9162.
[8] For example: a) S. A. Reiter, S. D. Nogai, K. Karaghiosoff, H. Schmidbaur, *J. Am. Chem. Soc.* **2004**, *126*, 15833; b) P. Kilian, A. M. Z. Slawin, J. D. Woollins, *Phosphorus Sulfur Silicon Relat. Elem.* **2004**, *179*, 999.
[9] W. Nakanishi, S. Hayashi, *Chem. Eur. J.* **2008**, *14*, 5645.
[10] A. Bondi, *J. Phys. Chem.* **1964**, *68*, 441.
[11] M. Bühl, F. R. Knight, A. Křístková, I. Malkin Ondík, O. L. Malkina, R. A. M. Randall, A. M. Z. Slawin, J. D. Woollins, *Angew. Chem.* **2013**, *125*, 2555; *Angew. Chem. Int. Ed.* **2013**, *52*, 2495.
[12] F. R. Knight, A. L. Fuller, M. Bühl, A. M. Z. Slawin, J. D. Woollins, *Chem. Eur. J.* **2010**, *16*, 7503.
[13] L. K. Aschenbach, F. R. Knight, R. A. M. Randall, D. B. Cordes, A. Baggott, M. Bühl, A. M. Z. Slawin, J. D. Woollins, *Dalton Trans.* **2012**, *41*, 3141.
[14] L. M. Diamond, F. R. Knight, K. S. Athukorala Arachchige, R. A. M. Randall, M. Bühl, A. M. Z. Slawin, J. D. Woollins, *Eur. J. Inorg. Chem.* **2014**, 1512.
[15] M. Oba, Y. Okada, M. Endo, K. Tanaka, K. Nishiyama, S. Shimada, W. Ando, *Inorg. Chem.* **2010**, *49*, 10680.
[16] a) W. Nakanishi, S. Hayashi, S. Toyota, *Chem. Commun.* **1996**, 371; b) W. Nakanishi, S. Hayashi, A. Sakaue, G. Ono, Y. Kawada, *J. Am. Chem. Soc.* **1998**, *120*, 3635; c) W. Nakanishi, S. Hayashi, S. Toyota, *J. Org. Chem.* **1998**, *63*, 8790; d) S. Hayashi, W. Nakanishi, *J. Org. Chem.* **1999**, *64*, 6688; e) W. Nakanishi, S. Hayashi, T. Uehara, *J. Phys. Chem. A* **1999**, *103*, 9906–9912; f) W. Nakanishi, S. Hayashi, *Phosphorus Sulfur Silicon Relat. Elem.* **2002**, *177*, 1833; g) W. Nakanishi, S. Hayashi, *J. Org. Chem.* **2002**, *67*, 38–48; h) S. Hayashi, W. Nakanishi, *Bull. Chem. Soc. Jpn.* **2008**, *81*, 1605; i) S. Hayashi, K. Yamane, W. Nakanishi, *Bioinorg. Chem. Appl.* **2009**, 347359; j) T. Nakai, M. Nishino, S. Hayashi, M. Hashimoto, W. Nakanishi, *Dalton Trans.* **2012**, *41*, 7485.
[17] P. Nagy, D. Szabó, I. Kapovits, Á. Kucsman, G. Argay, A. Kálmán, *J. Mol. Struct.* **2002**, *606*, 61.
[18] M. W. Stanford, F. R. Knight, K. S. Athukorala Arachchige, P. Sanz Camacho, S. E. Ashbrook, M. Bühl, A. M. Z. Slawin, J. D. Woollins, *Dalton Trans.* **2014**, *43*, 6548.
[19] P. Kilian, F. R. Knight, J. D. Woollins, *Chem. Eur. J.* **2011**, *17*, 2302.
[20] V. Balasubramaniyan, *Chem. Rev.* **1966**, *66*, 567.
[21] B. A. Chalmers, K. S. Athukorala Arachchige, J. K. D. Prentis, F. R. Knight, P. Kilian, A. M. Z. Slawin, J. D. Woollins, *Inorg. Chem.* **2014**, *53*, 8795.
[22] K. Wiberg, *Tetrahedron* **1968**, *24*, 1083.
[23] H. O. House, D. G. Koepsell, W. J. Campbell, *J. Org. Chem.* **1972**, *37*, 1003.
[24] a) N. Tanaka, T. Kasai, *Bull. Chem. Soc. Jpn.* **1981**, *54*, 3020; b) Y. Aso, K. Yui, T. Miyoshi, T. Otsubo, *Bull. Chem. Soc. Jpn.* **1988**, *61*, 2013; c) W. D. Neudorff, D. Lentz, M. Anibarro, A. D. Schlüter, *Chem. Eur. J.* **2003**, *9*, 2745.
[25] A. L. Fuller, L. A. S. Scott-Hayward, Y. Li, M. Bühl, A. M. Z. Slawin, J. D. Woollins, *J. Am. Chem. Soc.* **2010**, *132*, 5799.
[26] CrystalClear: Rigaku Corporation, **1999**. CrystalClear Software User's Guide, Molecular Structure Corporation, **2000**. J. W. Pflugrath, *Acta Crystallogr. D* **1999**, *55*, 1718.
[27] SIR2004: M. C. Burla, R. Caliandro, M. Camalli, B. Carrozzini, G. L. Cascarano, L. De Caro, C. Giacovazzo, G. Polidori, R. Spagna, **2005**.
[28] DIRDIF99: P. T. Beurskens, G. Admiraal, G. Beurskens, W. P. Bosman, R. de Gelder, R. Israel, J. M. M. Smits, **1999**. The DIRDIF-99 program system, Technical Report of the Crystallography Laboratory, University of Nijmegen, The Netherlands.
[29] CrystalStructure 4.1: Crystal Structure Analysis Package, Rigaku Corporation (**2000–2014**). Tokyo 196–8666, Japan.
[30] SHELX2013: G. M. Sheldrick, **2013**, University of Gottingen, Germany.
[31] a) J. Autschbach, T. Ziegler, *J. Chem. Phys.* **2000**, *113*, 936; b) J. Autschbach, *J. Chem. Phys.* **2008**, *129*, 094105.
[32] See for instance a) J. Autschbach, *Struct. Bonding* **2004**, *112*, 1; b) A. Bagno, G. Casella, G. Saielli, *J. Chem. Theory Comput.* **2006**, *2*, 37; c) F. Chen, G. M. Bernard, R. G. Cavell, R. McDonald, M. J. Ferguson, R. E. Wasylishen, *J. Am. Chem. Soc.* **2010**, *132*, 5479; d) S. Moncho, J. Autschbach, *J. Chem. Theory Comput.* **2010**, *6*, 223.

Received: October 10, 2014
Published online on December 22, 2014